EUROPEAN ORGANIZATION FOR NUCLEAR RESEARCH (CERN)

CERN-EP-2019-025
2019/07/30

CMS-HIG-18-014

Search for charged Higgs bosons in the $H^{\pm} \to \tau^{\pm}\nu_{\tau}$ decay channel in proton-proton collisions at $\sqrt{s} = 13\,\text{TeV}$

The CMS Collaboration*

Abstract

A search is presented for charged Higgs bosons in the $H^{\pm} \to \tau^{\pm}\nu_{\tau}$ decay mode in the hadronic final state and in final states with an electron or a muon. The search is based on proton-proton collision data recorded by the CMS experiment in 2016 at a center-of-mass energy of 13 TeV, corresponding to an integrated luminosity of 35.9 fb^{-1}. The results agree with the background expectation from the standard model. Upper limits at 95% confidence level are set on the production cross section times branching fraction to $\tau^{\pm}\nu_{\tau}$ for an $H^{\pm}$ in the mass range of 80 GeV to 3 TeV, including the region near the top quark mass. The observed limit ranges from 6 pb at 80 GeV to 5 fb at 3 TeV. The limits are interpreted in the context of the minimal supersymmetric standard model $m_{h}^{\text{mod-}}$ scenario.

"Published in the Journal of High Energy Physics as doi:10.1007/JHEP10(2019)142."

*See Appendix A for the list of collaboration members

1 Introduction

In 2012, the ATLAS and CMS experiments observed a resonance consistent with the Higgs boson with a mass of approximately 125 GeV at the CERN LHC [1–3], providing strong evidence for spontaneous symmetry breaking via the Brout–Englert–Higgs mechanism [4–9]. The observation was followed by precision measurements of the mass, couplings, and CP quantum numbers of the new boson, which were found to be consistent with the predictions of the standard model (SM) of particle physics [10–14].

Several extensions of the SM predict a more complex Higgs sector with several Higgs fields, yielding a spectrum of Higgs bosons with different masses, charges, and other properties. These models are constrained, but not excluded, by the measured properties of the 125 GeV boson. The observation of additional Higgs bosons would provide unequivocal evidence for the existence of physics beyond the SM. Two-Higgs-doublet models (2HDMs) predict five different Higgs bosons: two neutral CP-even particles h and H (with $m_{\mathrm{h}} \leq m_{\mathrm{H}}$), one neutral CP-odd particle A, and two charged Higgs bosons $\mathrm{H}^{\pm}$ [15].

The 2HDMs are classified into different types, depending on the coupling of the two Higgs doublets to fermions. This search is interpreted in the context of the "type II" 2HDM, where one doublet couples to down-type quarks and charged leptons, and the other to up-type quarks. The minimal supersymmetric standard model (MSSM) Higgs sector is a type II 2HDM [16]. At tree level, the Higgs sector of a type II 2HDM can be described with two parameters. In the context of $\mathrm{H}^{\pm}$ searches, they are conventionally chosen to be the mass of the charged Higgs boson ($m_{\mathrm{H}^{\pm}}$) and the ratio of the vacuum expectation values of the two Higgs doublets, denoted as $\tan\beta$. Charged Higgs bosons are also predicted by more complex models, such as triplet models [17–19].

The dominant production mechanism of the $\mathrm{H}^{\pm}$ depends on its mass. Examples of leading order (LO) diagrams describing the $\mathrm{H}^{\pm}$ production in 2HDM in different mass regions are shown in Fig. 1. Light $\mathrm{H}^{\pm}$, with a mass smaller than the mass difference between the top and the bottom quarks ($m_{\mathrm{H}^{\pm}} < m_{\mathrm{t}} - m_{\mathrm{b}}$), are predominantly produced in decays of top quarks (double-resonant top quark production, Fig. 1 left), whereas heavy $\mathrm{H}^{\pm}$ ($m_{\mathrm{H}^{\pm}} > m_{\mathrm{t}} - m_{\mathrm{b}}$) are produced in association with a top quark as $\mathrm{pp} \to \mathrm{tbH}^{\pm}$ (single-resonant top quark production, Fig. 1 middle). In the intermediate region near the mass of the top quark ($m_{\mathrm{H}^{\pm}} \sim m_{\mathrm{t}}$), the nonresonant top quark production mode (Fig. 1 right) also contributes and the full $\mathrm{pp} \to \mathrm{H}^{\pm}\mathrm{W}^{\mp}\mathrm{b}\bar{\mathrm{b}}$ process must be calculated in order to correctly account for all three production mechanisms and their interference [20].

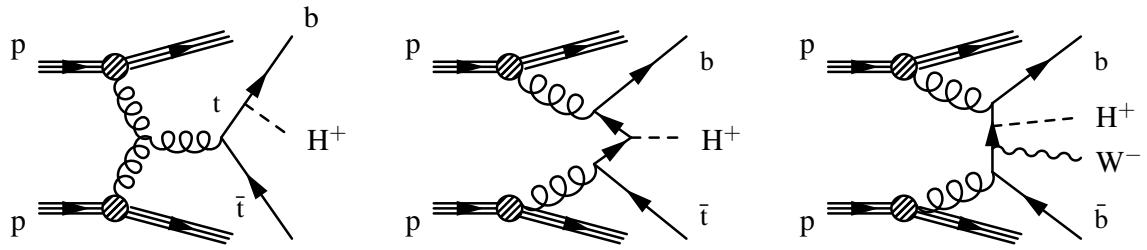

Figure 1: Leading order diagrams describing charged Higgs boson production. Double-resonant top quark production (left) is the dominant process for light $\mathrm{H}^{\pm}$, whereas the single-resonant top quark production (middle) dominates for heavy $\mathrm{H}^{\pm}$ masses. For the intermediate region ($m_{\mathrm{H}^{\pm}} \sim m_{\mathrm{t}}$), both production modes and their interplay with the nonresonant top quark production (right) must be taken into account. Charge-conjugate processes are implied.

In type II 2HDM, a light $H^{\pm}$ decays almost exclusively to a tau lepton and a neutrino. For the heavy $H^{\pm}$, the decay into top and bottom quarks ($H^{+} \to t\bar{b}$ and $H^{-} \to \bar{t}b$, together denoted as $H^{\pm} \to tb$) is dominant, but since the coupling of the $H^{\pm}$ to leptons is proportional to $\tan\beta$, the branching fraction to a tau lepton and a neutrino ($H^{+} \to \tau^{+}\nu_{\tau}$ and $H^{-} \to \tau^{-}\bar{\nu}_{\tau}$, together denoted as $H^{\pm} \to \tau^{\pm}\nu_{\tau}$) remains sizable for large values of $\tan\beta$.

Direct searches for $H^{\pm}$ have been performed at LEP [21], at the Fermilab Tevatron [22, 23], and by the LHC experiments. The ATLAS and CMS Collaborations have covered several $H^{\pm}$ decay channels, such as $\tau^{\pm}\nu_{\tau}$ [24–30], t b [28, 31, 32], c s [33, 34], c b [35] and $W^{\pm}Z$ [36, 37], in their previous searches at center-of-mass energies of 7, 8, or 13 TeV. Additionally, the ATLAS and CMS results on searches for additional neutral Higgs bosons have been interpreted in the 2HDM parameter space, constraining the allowed $H^{\pm}$ mass range as a function of $\tan\beta$ [38–41].

In this paper, a direct search for $H^{\pm}$ decaying into a tau lepton and a neutrino is presented, based on data collected at a center-of-mass energy of 13 TeV by the CMS experiment in 2016, corresponding to an integrated luminosity of 35.9 fb^{-1}. The search is conducted in three different final states, labeled in this paper as the hadronic final state (τ_{h} + jets, where τ_{h} denotes a hadronically decaying tau lepton), the leptonic final state with a τ_{h} (ℓ + τ_{h}), and the leptonic final state without a τ_{h} (ℓ + no τ_{h}). For the hadronic final state, events contain a τ_{h}, missing transverse momentum due to neutrinos, and additional hadronic jets from top quark decays and b quarks. The leptonic final state with a τ_{h} contains a single isolated lepton (electron or muon), missing transverse momentum, hadronic jets and a τ_{h}. The leptonic final state without a τ_{h} is defined in a similar way, except that events with a τ_{h} are rejected. In the leptonic final states, the lepton can originate either from the decays of the tau leptons from $H^{\pm}$ decays, or from a $W^{\pm}$ boson decay.

In each final state, events are further classified into different categories for statistical analysis. A transverse mass distribution is reconstructed in each category of each final state and used in a maximum likelihood fit to search for an $H^{\pm}$ signal. The $H^{\pm}$ mass range from 80 GeV to 3 TeV is covered in the search, including the intermediate mass range near m_{t}.

This paper is organized as follows. The CMS detector is briefly presented in Section 2. The methods used in event simulation and reconstruction are described in Sections 3 and 4, respectively. The event selection and categorization criteria are presented in Section 5, while Section 6 details the background estimation methods used in the analysis. Systematic uncertainties included in the analysis are described in Section 7. Finally, the results are presented in Section 8 and summarized in Section 9.

2 The CMS detector

The central feature of the CMS apparatus is a superconducting solenoid of 6 m internal diameter, providing a magnetic field of 3.8 T. Within the solenoid volume are a silicon pixel and strip tracker, a lead tungstate crystal electromagnetic calorimeter (ECAL), and a brass and scintillator hadron calorimeter, each composed of a barrel and two endcap sections. Forward calorimeters extend the pseudorapidity (η) coverage provided by the barrel and endcap detectors up to $|\eta| = 5$. Muons are detected in gas-ionization chambers embedded in the steel flux-return yoke outside the solenoid. Events of interest are selected using a two-tiered trigger system [42]. The first level, composed of custom hardware processors, uses information from the calorimeters and muon detectors to select events at a rate of around 100 kHz within a time interval of less than 4 μs. The second level, known as the high-level trigger (HLT), consists of a farm of processors running a version of the full event reconstruction software optimized for fast processing,

and reduces the event rate to around 1 kHz before data storage. A more detailed description of the CMS detector, together with a definition of the coordinate system used and the relevant kinematic variables, can be found in Ref. [43].

3 Event simulation

The signal samples for the light $H^{\pm}$ mass values from 80 to 160 GeV are generated at next-to-leading order (NLO) with the MADGRAPH5_aMC@NLO v2.3.3 [44] generator, assuming $H^{\pm}$ production via top quark decay ($pp \to H^{\pm}W^{\mp}b\bar{b}$). For the heavy $H^{\pm}$ mass range from 180 GeV to 3 TeV, the same approach is used except that $H^{\pm}$ production via $pp \to tbH^{\pm}$ is assumed. For the intermediate mass range from 165 to 175 GeV, the samples are generated at LO using the MADGRAPH5_aMC@NLO v2.3.3 with the model described in Ref. [20], which is available only at LO.

The effect of using LO instead of NLO samples is estimated by comparing kinematic distributions and final event yields from both types of samples in mass regions below (150–160 GeV) and above (180–220 GeV) the intermediate range. Significant differences are observed in some kinematic variables such as jet multiplicity, affecting the selection efficiency and the predicted final signal yield. Since the shapes of the final m_{T} distributions are found to be compatible between the LO and the NLO samples, a LO-to-NLO correction is performed by scaling the final signal event yield from each intermediate-mass sample. The overall effect of the correction is to scale down the signal event yield, resulting in more conservative results than would be obtained using LO samples without this correction.

The NLO/LO signal yield ratios are similar for all mass points within the 150–160 GeV and 180–200 GeV mass regions, but different between these two regions. Thus the correction factor for each final state and event category is calculated as an average over the NLO/LO ratios of the final event yields. This is done separately for the 150–160 GeV and 180–200 GeV regions, and the correction derived in the 150–160 GeV region is applied to the intermediate signal sample with $m_{\mathrm{H}^{\pm}} = 165$ GeV, for which $m_{\mathrm{H}^{\pm}} < m_{\mathrm{t}} - m_{\mathrm{b}}$ and the $H^{\pm}$ production is still dominated by top quark decays, while the correction derived in the 180–200 GeV region is applied to the 170 and 175 GeV samples with $m_{\mathrm{H}^{\pm}} > m_{\mathrm{t}} - m_{\mathrm{b}}$. For all signal samples up to $m_{\mathrm{H}^{\pm}} = 500$ GeV, MADSPIN [45] is used to model the $H^{\pm}$ decay, while PYTHIA 8.212 is used above 500 GeV.

In the leptonic final states, where accurate modeling of jet multiplicity is needed for the correct categorization of events, the MG5_aMC@NLO v2.2.2 generator [44] is used to simulate the $t\bar{t}$ events at NLO. In the hadronic final state, the statistical uncertainty in the final event yield needs to be minimized for reliable modeling of the m_{T} shape of the $t\bar{t}$ background, and thus a larger sample generated using POWHEG v2.0 [46–50] with FxFx jet matching and merging [51] is used to model this background. The POWHEG v2.0 generator is used to model single top quark production via t-channel and t W production [52, 53], while the MADGRAPH5_aMC@NLO v2.2.2 generator is used for the s-channel production. The value of m_{t} is set to 172.5 GeV for all $t\bar{t}$ and single top quark samples. The W +jets and Z/γ^* events are generated at LO using MADGRAPH5_aMC@NLO v2.2.2 with up to four noncollinear partons in the final state [54]. The diboson processes (WW, WZ, ZZ) are simulated using PYTHIA 8.212.

The simulated samples are normalized to the theoretical cross sections for the corresponding processes. For the $t\bar{t}$ background and the single top quark background in the s and t W channels, the cross sections are calculated at next-to-NLO precision [55, 56]. NLO precision calculations are used for single top quark production in the t channel, and for the W +jets, Z/γ^*, and diboson processes [56–59].

For all simulated samples, the NNPDF3.0 parton distribution functions (PDFs) [60] are used, and the generators are interfaced with PYTHIA 8.212 to model the parton showering, fragmentation, and the decay of the tau leptons. The PYTHIA parameters affecting the description of the underlying event are set to the CUETP8M1 tune [61] for all processes except $\mathrm{t\bar{t}}$, for which a customized CUETP8M2T4 tune [62] is used.

Generated events are processed through a simulation of the CMS detector based on the GEANT4 v9.4 software [63], and they are reconstructed following the same algorithms that are used for data. The effect of additional soft inelastic proton-proton (pp) interactions (pileup) is modeled by generating minimum bias collision events with PYTHIA and mixing them with the simulated hard scattering events. The effects from multiple inelastic pp collisions occurring per bunch crossing (in-time pileup), as well as the effect of inelastic collisions happening in the preceding and subsequent bunch crossings (out-of-time pileup) are taken into account. The simulated events are weighted such that the final pileup distribution matches the one observed in data. For the data collected in 2016, an average of approximately 23 interactions per bunch crossing was measured.

4 Event reconstruction

Event reconstruction is based on the particle-flow (PF) algorithm [64] that aims to reconstruct and identify each individual particle in an event with an optimized combination of information from the various elements of the CMS detector. The output of the PF algorithm is a set of PF candidates, classified into muons, electrons, photons, and charged and neutral hadrons.

The collision vertices are reconstructed from particle tracks using the deterministic annealing algorithm [65]. The reconstructed vertex with the largest value of the physics-object transverse momentum squared (p_{T}^2) sum is taken to be the primary p p interaction vertex. The physics objects in this case are the jets, clustered using the anti-k_{T} jet finding algorithm [66, 67] with the tracks assigned to the vertex as inputs, and the associated missing transverse momentum, calculated as the negative vector sum of the p_{T} of those jets. All other reconstructed vertices are attributed to pileup.

Electrons are reconstructed and their momentum is estimated by combining the momentum measurement from the tracker at the interaction vertex with the energy measurement in the ECAL. The energy of the corresponding ECAL cluster and the energy sum of all bremsstrahlung photons spatially compatible with originating from the electron tracks are taken into account. The momentum resolution for electrons with $p_{\mathrm{T}} \approx 45\,\mathrm{GeV}$ from $\mathrm{Z} \to \mathrm{ee}$ decays ranges from 1.7% for nonshowering electrons in the barrel region to 4.5% for showering electrons in the endcaps [68]. In addition, electrons are required to pass an identification requirement based on a multivariate discriminant that combines several variables describing the shape of the energy deposits in the ECAL, as well as the direction and quality of the associated tracks [69]. A tight working point with 88% identification efficiency for $\mathrm{t\bar{t}}$ events is used to select events with an electron, while a loose working point with 95% efficiency is used to veto events with one or several electrons, depending on the final state.

Muons are identified as tracks in the central tracker, consistent with either a track or several hits in the muon chambers, and associated with calorimeter deposits compatible with the muon hypothesis [70]. The momenta of muons are obtained from the curvatures of the corresponding tracks. Contributions from other particles misidentified as muons are suppressed with a discriminant based on the track fit quality. Two working points as defined in Ref. [70] are used: a medium working point with 97% identification efficiency is used to select events with a muon,

while a loose working point with >99% identification efficiency is used for vetoing muons.

The background contributions from nonprompt and misidentified leptons are suppressed by requiring the leptons to be isolated from hadronic activity in the event. For this purpose, an isolation discriminant is defined as the p_T sum of the PF candidates in a cone around the lepton, divided by the p_T of the lepton. For optimal performance across the lepton momentum range, the cone size is varied with the lepton p_T as $\Delta R = \sqrt{(\Delta\eta)^2 + (\Delta\phi)^2} = 10\,\text{GeV}/\min(\max(p_T, 50\,\text{GeV}), 200\,\text{GeV})$, where $\Delta\phi$ denotes a difference in azimuthal angle, leading to cone radii from 0.05 to 0.20. A tight (loose) isolation criterion with discriminant < 0.1 (0.4) is used in lepton selection (veto).

For each event, hadronic jets are clustered from the reconstructed PF candidates using the infrared and collinear safe anti-k_T algorithm [66, 67] with a distance parameter of 0.4. The jet momentum is determined as the vectorial sum of all particle momenta in the jet, and is found from simulation to be within 5 to 10% of the true momentum over the whole p_T spectrum and detector acceptance. Pileup can contribute additional tracks and calorimetric energy deposits to the jet momentum. To mitigate this effect, tracks identified as originating from pileup vertices are discarded and an offset correction is applied to correct for remaining contributions. Jet energy corrections are derived from simulation to bring the measured response of jets to that of particle level jets on average. In situ measurements of the momentum balance in dijet, photon + jet, Z + jet, and multijet events are used to account for any residual differences in jet energy scale between data and simulation [71]. The jet energy resolution amounts typically to 15% at 10 GeV, 8% at 100 GeV, and 4% at 1 TeV [72]. Additional selection criteria are applied to each jet to remove jets potentially dominated by anomalous contributions from various subdetector components or reconstruction failures.

Jets originating from the hadronization of b quarks (b jets) are identified using the combined secondary vertex algorithm [73, 74], which uses information on the decay vertices of long-lived hadrons and the impact parameters of charged particle tracks as input to a neural network discriminant. The working point is chosen such that the probability to misidentify jets originating from light-flavor quarks or gluons (c quarks) as b jets is 1% (12%), corresponding to 63% efficiency for the selection of genuine b jets in $\mathrm{t\bar{t}}$ events. Simulated samples are corrected for differences in b jet identification and misidentification efficiency compared to the data.

The τ_h are reconstructed with the hadron-plus-strips algorithm [75, 76], which uses clustered anti-k_T jets as seeds. The hadron-plus-strips algorithm reconstructs different τ decay modes with one charged pion and up to two neutral pions (one-prong), or three charged pions (three-prong). Since neutral pions decay promptly to a photon pair, they are reconstructed by defining strips of ECAL energy deposits in the η–ϕ plane. The τ_h candidates are rejected if they are consistent with the hypothesis of being muons or electrons misidentified as τ_h. The jets originating from the hadronization of quarks or gluons misidentified as τ_h are suppressed using a multivariate discriminant [76]. It combines information on τ_h isolation, based on the surrounding hadronic activity, and on its lifetime, inferred from the tracks of the τ_h decay products. A loose working point is used for this discriminant, corresponding to ≈50% identification efficiency, determined from $Z/\gamma^* \to \tau^+\tau^-$ events, and 3×10^{-3} probability for misidentifying a jet as a τ_h, determined from quantum chromodynamics (QCD) multijet events. A correction to the energy scale is derived using $e\tau_h$ and $\mu\tau_h$ final states of $Z/\gamma^* \to \tau^+\tau^-$ events [76] and applied in simulated samples.

The missing transverse momentum ($\vec{p}_T^{\,\text{miss}}$) is defined as the negative vector sum of the p_T of all reconstructed PF candidates [77]. The energy scale corrections applied to jets and τ_h are propagated to the $\vec{p}_T^{\,\text{miss}}$.

The transverse mass is defined as

$$m_{\mathrm{T}}(\tau_{\mathrm{h}}/\ell) = \sqrt{2p_{\mathrm{T}}(\tau_{\mathrm{h}}/\ell)p_{\mathrm{T}}^{\mathrm{miss}}(1-\cos\Delta\phi(\vec{p}_{\mathrm{T}}(\tau_{\mathrm{h}}/\ell),\vec{p}_{\mathrm{T}}^{\mathrm{miss}}))}, \quad (1)$$

where ℓ is a generic symbol used to label the electron or muon present in the leptonic final states, while the leading τ_{h} is used in the m_{T} in the hadronic final state.

5 Event selection

The search is conducted in three exclusive final states:

- τ_{h} + jets: hadronic final state (events with an electron or a muon are vetoed);
- ℓ + τ_{h}: leptonic final state with a hadronically decaying tau lepton (events with additional electrons or muons are vetoed); and
- ℓ + no τ_{h}: leptonic final state without a hadronically decaying tau lepton (events with a τ_{h} or additional electrons or muons are vetoed).

In the low-$m_{\mathrm{H}^{\pm}}$ region, below m_{t}, the sensitivity of the hadronic final state is limited by the relatively high trigger thresholds, making the leptonic final states most sensitive for the $\mathrm{H}^{\pm}$ signal. In the high-$m_{\mathrm{H}^{\pm}}$ region, above m_{t}, the hadronic final state dominates the sensitivity, since the selection efficiency is higher as a result of more inclusive jet multiplicity requirements.

The event selection and categorization strategies are chosen separately for each final state to efficiently discriminate against the background events, while ensuring a sufficient signal selection efficiency.

5.1 Hadronic final state (τ_{h} + jets)

An HLT algorithm requiring the presence of a τ_{h} candidate and trigger-level missing transverse momentum estimated from calorimeter information ($p_{\mathrm{T}}^{\mathrm{miss,calo}}$) is used to select the events for offline analysis. The trigger requires the τ_{h} candidate to be loosely isolated with $p_{\mathrm{T}} > 50\,\mathrm{GeV}$ and $|\eta| < 2.1$, and with a leading track transverse momentum $p_{\mathrm{T}}^{\mathrm{track}} > 30\,\mathrm{GeV}$. The $p_{\mathrm{T}}^{\mathrm{miss,calo}}$ is required to be larger than 90 GeV.

The trigger efficiencies for the τ_{h} and $p_{\mathrm{T}}^{\mathrm{miss,calo}}$ requirements are measured separately. The efficiency of the τ_{h} part of the trigger is determined with the tag-and-probe technique [78], using $\mathrm{Z}/\gamma^{*} \to \tau^{+}\tau^{-}$ events with one hadronic and one muonic tau lepton decay. The efficiency is found to vary between 50 and 100%, as a function of p_{T} and η of the τ_{h}. The efficiency of the $p_{\mathrm{T}}^{\mathrm{miss,calo}}$ part of the trigger is measured from events with a signal-like topology selected with a single-τ_{h} trigger, resulting in efficiencies between 10 and 100%, depending on the value of the $p_{\mathrm{T}}^{\mathrm{miss}}$. The simulated events are corrected to match the trigger efficiencies measured in the data.

In the offline selection, low thresholds for the p_{T} of the reconstructed τ_{h} and $p_{\mathrm{T}}^{\mathrm{miss}}$ are needed to maximize the sensitivity for light $\mathrm{H}^{\pm}$. Thus selection criteria identical to those in the HLT are applied to the reconstructed τ_{h} candidate and to the $p_{\mathrm{T}}^{\mathrm{miss}}$. The one-prong τ_{h} candidates, corresponding to τ decays into a charged pion and up to two neutral pions, are selected for further analysis. Events are required to contain at least three jets with $p_{\mathrm{T}} > 30\,\mathrm{GeV}$ and $|\eta| < 4.7$, separated from the reconstructed τ_{h} by $\Delta R > 0.5$. At least one of the jets is required to pass the b jet identification with $|\eta| < 2.4$. Any event with isolated electrons (muons) with $p_{\mathrm{T}} > 15(10)\,\mathrm{GeV}$, $|\eta| < 2.5$, and passing the loose identification and isolation criteria is rejected.

To suppress the background from QCD multijet events with a jet misidentified as a τ_{h}, an additional selection based on $\Delta\phi(\tau_{\mathrm{h}}, p_{\mathrm{T}}^{\mathrm{miss}})$ and $\Delta\phi(\mathrm{jet}_{n}, p_{\mathrm{T}}^{\mathrm{miss}})$ is applied, where the index n runs

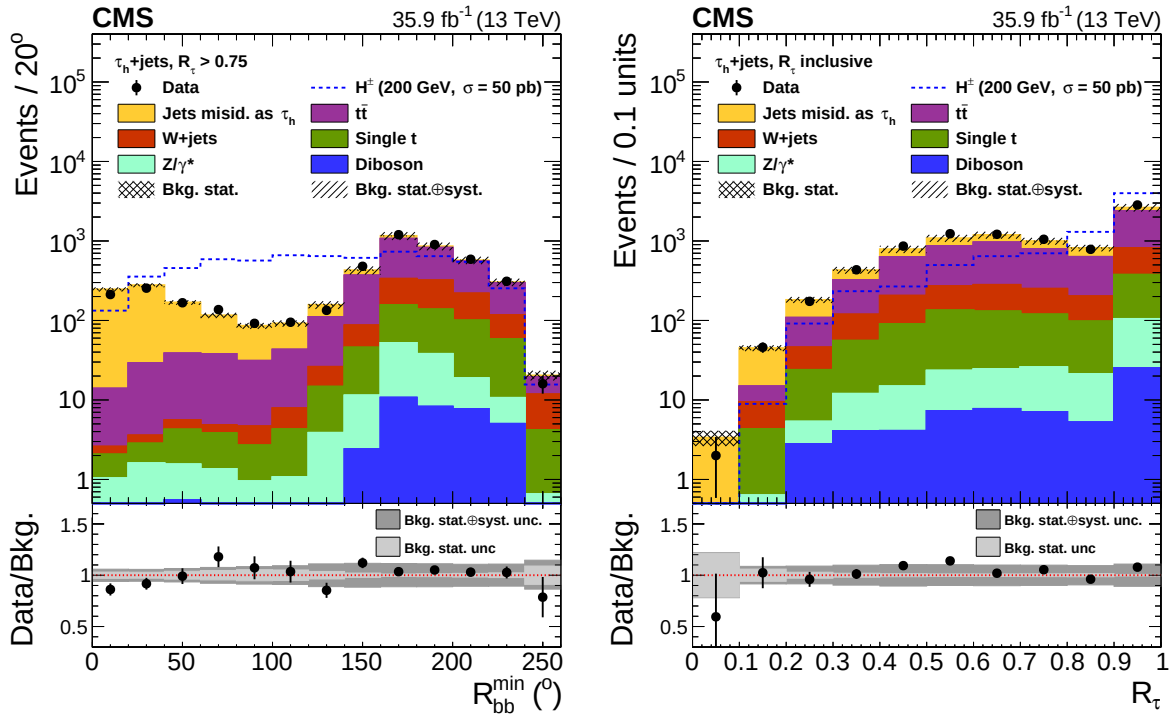

Figure 2: The distribution of the angular discriminant R_{bb}^{min} after all other selections including the $R_\tau = p_T^{track}/p_T^{\tau_h} > 0.75$ requirement have been applied (left), and the distribution of the R_τ variable used for categorization after all other selections including the $R_{bb}^{min} > 40^\circ$ requirement have been applied (right).

over the three highest p_T jets (jet$_n$) in the event. QCD multijet events passing the previous selection steps typically contain a hadronic jet misidentified as a τ_h, another hadronic jet recoiling in the opposite direction, and $\vec{p}_T^{miss}$ arising from the mismeasurement of the jet momenta. These events can be suppressed with an angular discriminant defined as

$$R_{bb}^{min} = \min_n \left\{ \sqrt{\left(180^\circ - \Delta\phi(\tau_h, \vec{p}_T^{miss})\right)^2 + \left(\Delta\phi(\text{jet}_n, \vec{p}_T^{miss})\right)^2} \right\}. \quad (2)$$

The selected events are required to have $R_{bb}^{min} > 40^\circ$. The distribution of the R_{bb}^{min} variable after all other selections is shown in Fig. 2 (left).

The selected events are classified into two categories based on the value of the variable $R_\tau = p_T^{track}/p_T^{\tau_h}$, reflecting the helicity correlations emerging from the opposite polarization states of the tau leptons originating from $W^\pm$ and $H^\pm$ decays [79]. The distribution of the R_τ variable is shown in Fig. 2 (right). After all other selections, most of the signal events have a large value of R_τ, and the high-R_τ category provides a good signal-to-background ratio. For large $m_{H^\pm}$ values, the signal events are more evenly distributed between the two categories, so inclusion of the background-dominated low-R_τ category in the statistical analysis further improves the sensitivity for the heavy $H^\pm$. Separating the two categories at $R_\tau = 0.75$ maximizes the signal sensitivity across the $m_{H^\pm}$ range.

5.2 Leptonic final state with a hadronically decaying tau lepton (ℓ + τ_h)

Single-lepton trigger algorithms are used for the online selection of events with isolated electrons or muons. Several HLT algorithms for electron (muon) selection with different thresholds

starting from 27 (24) GeV, with $|\eta| < 2.1$ (2.4) and with different isolation criteria, are used in *or* combination to maximize the efficiency across the lepton p_T range.

In the offline selection, electrons (muons) are required to have $p_T > 35(30)$ GeV and $|\eta| < 2.1(2.4)$ because of trigger constraints. Electrons (muons) are required to pass the tight (medium) identification and tight isolation requirements. Events with any additional electrons (muons) with $p_T > 10$ GeV and $|\eta| < 2.1(2.4)$ that pass the loose identification and isolation criteria are vetoed. Efficiencies for online and offline identification of leptons are measured, and the simulated events are corrected to match the efficiencies observed in data. The presence of a τ_h is required, with $p_T > 20$ GeV, $|\eta| < 2.3$, and with a ΔR separation of at least 0.5 with respect to the lepton.

One, two, or three jets are required with $p_T > 30$ GeV and $|\eta| < 2.4$, separated from the lepton and the τ_h by $\Delta R > 0.5$. At least one of the jets is required to pass the b jet identification. To suppress the background from jets misidentified as τ_h, the p_T^{miss} is required to be at least 70 GeV. The background contribution from events with muons originating from b hadron decays is suppressed by requiring $\Delta\phi(\ell, \vec{p}_T^{miss})$ to exceed 0.5.

The selected events are classified into several categories for statistical analysis. Three categories are defined based on the jet multiplicity and the number of jets passing the b jet identification: 1j1b (one jet that is also identified as a b jet), $\geq$2j1b, and $\geq$2j$\geq$2b. A second categorization is performed in bins of p_T^{miss}: 70–100, 100–150, and >150 GeV. Together with the separate electron and muon final states, this results in 18 categories.

The signal-to-background ratio in different categories varies with $H^\pm$ mass, as jet categories with two jets and high p_T^{miss} become more sensitive for higher $m_{H^\pm}$ values. The background-enriched categories allow a precise determination of the background yields with a fit to data and extrapolation of this information to signal regions. The categorization is found to improve the expected sensitivity significantly, especially in the low-$m_{H^\pm}$ region, where efficient discrimination against backgrounds is essential.

5.3 Leptonic final state without a hadronically decaying tau lepton (ℓ + no τ_h)

The event selection criteria for the ℓ + no τ_h final state are identical to those described in Section 5.2 for the ℓ + τ_h final state, except for the following requirements. An event is vetoed if it contains a τ_h with $p_T > 20$ GeV, $|\eta| < 2.3$, and with a ΔR separation of at least 0.5 with respect to the lepton. Two or three jets are required, each jet separated from the lepton by $\Delta R > 0.5$. Higher jet multiplicities are not selected, because they are expected to be more sensitive in searches for other $H^\pm$ decay modes, such as $H^\pm \to tb$. At least one of the jets is required to pass the b jet identification.

The number of QCD multijet events with jets misidentified as leptons is reduced to a negligible level by requiring a high p_T^{miss} of >100 GeV and by applying the following angular selections:

- $\Delta\phi(\ell, \vec{p}_T^{miss}) > 0.5$;
- $\Delta\phi(\text{leading jet}, \vec{p}_T^{miss}) > 0.5$; and
- $\min(\Delta\phi(\ell, \text{jet}_n)) < \pi - 0.5$,

where jet_n refers to any of the selected jets in the events. The first criterion is identical to the one applied in the ℓ + τ_h final state against muons from b hadron decays whereas the second discriminates efficiently against the QCD multijet background. The last requirement is designed to reject background events where all the jets are back-to-back with respect to the selected lepton.

Table 1: A summary of the event selection criteria applied in each final state. The electrons, muons, τ_h candidates and jets are required to be separated from each other by $\Delta R > 0.5$ in all final states. The † symbol means that the selection is identical between ℓ + τ_h and ℓ + no τ_h final states. In all final states, events with additional electrons or muons are vetoed as detailed in Section 5. In this table, "b jets" refers to all jets passing the b jet identification, and jet$_n$ refers to any of the selected jets.

Selection	τ_h + jets	$\ell + \tau_h$	ℓ + no τ_h
Trigger	$\tau_h + p_T^{miss,calo}$	single e or single μ	†
Number of τ_h candidates	≥ 1	≥ 1	0
τ_h p_T	$p_T > 50\,GeV$, $p_T^{track} > 30\,GeV$	$p_T > 20\,GeV$	—
τ_h $\lvert\eta\rvert$	$\lvert\eta\rvert < 2.1$	$\lvert\eta\rvert < 2.3$	—
Number of electrons and muons	0	1e or 1 μ (exclusively)	†
Electron p_T	—	$p_T > 35\,GeV$	†
Ekectron $\lvert\eta\rvert$	—	$\lvert\eta\rvert < 2.1$	†
Muon p_T	—	$p_T > 30\,GeV$	†
Muon $\lvert\eta\rvert$	—	$\lvert\eta\rvert < 2.4$	†
Number of jets (incl. b jets)	≥ 3 jets	1–3 jets	2–3 jets
Jet p_T	$p_T > 30\,GeV$	$p_T > 30\,GeV$	†
Jet $\lvert\eta\rvert$	$\lvert\eta\rvert < 4.7$	$\lvert\eta\rvert < 2.4$	†
Number of b jets	≥ 1 b jets	1–3 b jets	†
b jet $\lvert\eta\rvert$	$\lvert\eta\rvert < 2.4$	$\lvert\eta\rvert < 2.4$	†
p_T^{miss}	$p_T^{miss} > 90\,GeV$	$p_T^{miss} > 70\,GeV$	$p_T^{miss} > 100\,GeV$
Angular selections	$R_{bb}^{min} > 40^\circ$	$\Delta\phi(\ell, p_T^{miss}) > 0.5$ (ℓ = e or μ)	$\Delta\phi(\ell, \vec{p}_T^{miss}) > 0.5$, $\Delta\phi$(leading jet, $\vec{p}_T^{miss}$) > 0.5, $\min(\Delta\phi(\ell, \text{jet}_n)) < \pi - 0.5$

To further enhance the signal sensitivity and to constrain the backgrounds, a similar categorization as in the ℓ + τ_h final state is established. Four categories are used based on jet multiplicity and the number of jets passing the b jet identification: 2j1b, 2j2b, 3j1b, and 3j$\geq$2b, followed by two categories in p_T^{miss}: 100–150 and >150 GeV. Together with the separate electron and muon final states, this results in 16 categories.

An overview of the event selection criteria in all three final states is shown in Table 1.

6 Background estimation

The dominant background processes in the hadronic final state are QCD multijet and $t\bar{t}$ production. Other backgrounds are single top quark production, W boson production in association with jets, Z/γ^* processes, and diboson production. We refer to $t\bar{t}$ and single top quark events as "top events", and to W +jets, Z/γ^*, and diboson events as "electroweak events". The backgrounds from events containing either a genuine τ_h or an electron or a muon misidentified as a τ_h are estimated from simulation, while the background from jets misidentified as a τ_h is estimated from data. The correct identification or misidentification of a τ_h is determined by requiring a generator-level tau lepton to match with the reconstructed τ_h within a ΔR cone of 0.1.

In the events where a jet is misidentified as a τ_h (denoted as jet $\to \tau_h$), QCD multijet production is the dominant process. The jet $\to \tau_h$ background is estimated using a control sample enriched in jets misidentified as τ_h, obtained by inverting the offline τ_h isolation requirement used for signal selection. The contamination of the control region from electroweak/top events with a genuine τ_h or a lepton misidentified as a τ_h is estimated from the simulation and subtracted from the control sample. The difference in selection efficiency between signal and control re-

gions is corrected by normalizing the control sample with *fake factors*, calculated at an early stage of event selection (i.e. before applying b jet identification, offline selection on $p_{\mathrm{T}}^{\mathrm{miss}}$ or the angular selections), where a possible signal does not stand out from the large background yield. To account for the correlation between the p_{T} of the τ_{h} and $p_{\mathrm{T}}^{\mathrm{miss}}$ as well as geometrical differences in detector response, the measurement is performed in bins of p_{T} and $|\eta|$ of the τ_{h}.

The jet $\rightarrow \tau_{\mathrm{h}}$ background consists of two components: the QCD multijet events and electroweak/top events with jets misidentified as τ_{h}. The jets in these two background components have different quark and gluon composition implying different tau fake factors. Thus the fake factors for misidentified τ_{h} from the QCD multijet events and for misidentified τ_{h} from electroweak/top events are estimated separately. The fake factor for the QCD multijet events is defined as the ratio of the QCD multijet event yields in signal and control regions. The QCD multijet event yield in the control region is estimated by subtracting the simulated electroweak/top contribution (both genuine and non-genuine τ_{h} events) from data. To estimate the contribution of the QCD multijet events in the signal region, a binned maximum likelihood fit of $p_{\mathrm{T}}^{\mathrm{miss}}$ templates to data is performed, using the fraction of the QCD multijet events as a fit parameter. The templates describe the expected shape of the $p_{\mathrm{T}}^{\mathrm{miss}}$ distribution for each background component prior to the fit. The $p_{\mathrm{T}}^{\mathrm{miss}}$ shape of the QCD multijet events is assumed to be similar in the signal and control regions, so the shape observed in the control region is used as the fit template. The template for electroweak/top events is obtained directly from simulation. The fake factor for electroweak/top events is also estimated from simulation as the ratio of event yields in signal and control regions. Finally, the overall normalization factor of the control sample (as a function of the p_{T} and $|\eta|$ of the τ_{h}) is determined as a weighted sum of the two fake factors, where the weight corresponds to the relative fractions of the QCD multijet and electroweak/top events in the control region after all selections. A closure test is performed by comparing the background predictions obtained with the above method to data in a signal-depleted validation region. The validation region is defined similarly to the signal region, except that events with jets passing the b jet identification are vetoed.

In the leptonic final states, the dominant background is $\mathrm{t\bar{t}}$ production in which the semileptonic $\mathrm{t\bar{t}}$ decays are dominant in the ℓ + no τ_{h} final state and the dilepton $\mathrm{t\bar{t}}$ decays are dominant in the ℓ + τ_{h} final state. Minor backgrounds include single top quark, W +jets, Z/γ^{*}, and diboson production. The QCD multijet background is suppressed to a negligible level with tight angular selections and $p_{\mathrm{T}}^{\mathrm{miss}}$ requirements. All backgrounds in the two leptonic final states are estimated from simulation.

7 Systematic uncertainties

A summary of uncertainties incorporated in the analysis is given in Table 2, where the effects of the different uncertainties on the final event yields are shown. For the uncertainties common to all final states, the variations in the yields are similar across the final states. Some of them affect only the final event yield for a given signal or background process, whereas others also modify the shape of the final m_{T} distributions. The uncertainties from different sources are assumed to be uncorrelated. Each uncertainty is treated as 100% correlated among the signal and background processes, except for the few special cases mentioned in the following.

The simulated events are corrected to match the online and offline selection efficiencies measured in data. For the trigger used in the τ_{h} + jets final state, the correction depends on the p_{T} of the τ_{h} and $p_{\mathrm{T}}^{\mathrm{miss}}$, so the corresponding uncertainty is taken into account as a shape uncertainty.

In the ℓ + τ_{h} and ℓ + no τ_{h} final states, the online selection with single-lepton triggers is in-

Table 2: Effect of systematic uncertainties on the final event yields in per cent, prior to the fit, summed over all final states and categories. For the $H^{\pm}$ signal, the values for $m_{H^{\pm}} = 200\,\text{GeV}$ are shown.

Source	Shape	$H^{\pm}$ (200 GeV)	Jets $\to \tau_h$	$t\bar{t}$	Single t	Electroweak
$\tau_h + p_T^{miss}$ trigger efficiency	✓	1.4	2.0	0.2	0.2	0.2
τ_h identification	✓	1.8	0.6	1.1	1.0	0.9
Lepton selection efficiency		2.3	—	2.7	2.7	2.7
Jet energy scale and resolution	✓	4.7	0.4	5.1	9.2	13.4
τ_h energy scale	✓	0.2	0.6	< 0.1	< 0.1	< 0.1
Unclustered p_T^{miss} energy scale	✓	2.6	< 0.1	3.2	5.2	7.2
b jet identification	✓	3.6	0.8	3.1	3.4	13.8
Integrated luminosity		2.5	0.4	2.5	2.5	2.5
Pileup	✓	1.1	< 0.1	0.8	1.2	4.0
Jets misid. as τ_h estimation	✓	—	6.1	—	—	—
Cross section (scales, PDF)		—	0.8	5.5	5.3	3.6
Top quark mass		—	0.4	2.7	2.2	—
Acceptance (scales, PDF)		5.1	0.5	2.8	2.8	6.8
$t\bar{t}$ parton showering		—	—	6.1	—	—
Total		9.4	6.6	12.1	13.5	22.7

corporated into the overall lepton selection efficiency and the corresponding normalization uncertainty.

The systematic uncertainties in identification and isolation efficiencies for τ_h, electron, and muon candidates are taken into account. The agreement of the τ_h identification efficiency between data and simulated samples is measured using the tag-and-probe technique [76]. The uncertainty in the measurement is 5%. It is incorporated as a normalization uncertainty for all events with genuine tau leptons, and anticorrelated between the ℓ + no τ_h final state and the final states with a τ_h. For the τ_h with large p_T, an additional uncertainty of $^{+5}_{-35}\% p_T$ / TeV is applied in the hadronic final state as a shape uncertainty to account for possible differences arising in the extrapolation of the measured efficiencies to the high-p_T range. Simulated events with an electron or a muon misidentified as a τ_h are weighted to obtain the misidentification rates measured in data. The corrections are applied as a function of η and the corresponding uncertainties are propagated to m_T distributions and incorporated as shape uncertainties.

For the selection of electrons (muons), the combined uncertainty in online selection and offline identification is 3 (4)%. For leptons vetoed with loose identification and isolation criteria the effect of this uncertainty in the final event yield is typically only 0.3%. Both effects are included as normalization uncertainties.

The systematic uncertainties related to the calibration of energy measurement for jets, τ_h and p_T^{miss} are considered as shape uncertainties. The uncertainties in the jet energy scale and jet energy resolution are specified as a function of jet p_T and η. The uncertainty in the τ_h energy scale is $\pm 1.2\%$ for $p_T < 400\,\text{GeV}$ and $\pm 3\%$ otherwise [76]. The variations of the jet and τ_h energy scales are propagated to $\vec{p}_T^{miss}$, for which the uncertainties arising from the unclustered energy deposits in the detector are also included. The uncertainty in the lepton energy scale is negligible for this analysis. Correcting the b jet identification and misidentification efficiencies in simulated samples affects the final m_T shapes, so the related uncertainties are considered as shape uncertainties [74].

The systematic uncertainty due to the pileup modeling is obtained by shifting the mean of the

total inelastic pp production cross section by $\pm 5\%$ around its nominal value [80], and propagating the difference to the final m_{T} distributions as a shape uncertainty.

The uncertainty in the measurement of the integrated luminosity is 2.5% [81].

The uncertainties related to the jet $\to \tau_{\mathrm{h}}$ background measurement in the hadronic final state are included. The statistical uncertainties in the data and simulated samples used to determine the fake factors are propagated into the final m_{T} distributions as a normalization uncertainty. The limited statistical precision of samples in the signal and control region after all selections can lead to a difference in m_{T} shapes between the two regions. This effect is estimated and incorporated as a shape uncertainty. As the jet $\to \tau_{\mathrm{h}}$ background is estimated by subtracting simulated events (electroweak/top contribution) from the control data sample, all uncertainties related to the simulated samples are propagated to this background. These uncertainties are scaled to correspond to the contribution from simulated events in the control region after all selections, and anticorrelated between the jet $\to \tau_{\mathrm{h}}$ background and the other background processes.

The reference cross sections used to normalize each simulated background process are varied within their theoretical uncertainties related to the choice of renormalization and factorization (RF) scales and PDFs [82]. For $\mathrm{t\bar{t}}$ and single top quark processes, the effect of m_{t} on the cross sections is considered by varying m_{t} by 1.0 GeV around the nominal value of 172.5 GeV. Theoretical uncertainties in the acceptance of signal and background events are determined by varying the RF scales and PDFs [82]. For the RF uncertainties, the RF scales are varied by factors of 0.5 and 2, excluding the extreme variations where one scale is varied by 0.5 and the other one by 2. The envelope of the six variations is used to determine the total uncertainty. The cross section and acceptance uncertainties are uncorrelated between different background processes.

The uncertainty arising from the parton shower modeling is included for the dominant $\mathrm{t\bar{t}}$ background in the leptonic final states. Four parton showering variations are included by perturbing the initial- and final-state parameters [83], the matching of jets from matrix element calculations and from parton shower, and the underlying event tune [62]. The parton shower uncertainties are derived in each category and are applied as normalization uncertainties, uncorrelated between categories. The leptonic final states are sensitive to the parton shower modeling due to the event categorization based on the jet multiplicity. In the hadronic final state, the event selection is inclusive in jet multiplicity and thus this uncertainty is neglected.

For the intermediate-mass signal samples, an additional normalization uncertainty is assigned to incorporate the statistical uncertainties of the samples used in the calculation of the LO-to-NLO correction factors.

The statistical uncertainties related to the finite number of events in the final m_{T} distributions are taken into account using the Barlow–Beeston method [84].

8 Results

A simultaneous binned maximum likelihood fit is performed over all the categories in the three final states. In total, 36 m_{T} distributions (two from the τ_{h} + jets final state, 18 from the ℓ + τ_{h} final state, and 16 from the ℓ + no τ_{h} final state) are fitted. The distributions are binned according to the statistical precision of the samples, separately for each category. This leads to wider bins in the tail of the distributions, such that the last bin extends to 5 TeV. The systematic uncertainties are incorporated as nuisance parameters in the likelihood. They are profiled in the fit

Table 3: Number of expected and observed events for the three final states after all selections, summed over all categories in each final state. For background processes, the event yields after a background-only fit and the corresponding uncertainties are shown. For the $H^{\pm}$ mass hypotheses of 100, 200, and 2000 GeV, the signal yields are normalized to an $H^{\pm}$ production cross section of 1 pb and the total systematic uncertainties (prior to the fit) are shown.

Process	τ_h + jets	ℓ + τ_h	ℓ + no τ_h
Jets misid. as τ_h	4619 ± 35	—	—
$t\bar{t}$	1455 ± 13	30560 ± 470	174740 ± 350
Single t	801 ± 13	3006 ± 49	26130 ± 260
Electroweak	1739 ± 18	2760 ± 37	52310 ± 220
Total expected from the SM	8614 ± 42	36320 ± 500	253190 ± 400
Observed	8647	36277	253236
$H^{\pm}$ signal, $m_{H^{\pm}} = 100$ GeV	20 ± 3	160 ± 20	241 ± 26
$H^{\pm}$ signal, $m_{H^{\pm}} = 200$ GeV	156 ± 22	327 ± 37	682 ± 61
$H^{\pm}$ signal, $m_{H^{\pm}} = 2000$ GeV	1630 ± 310	369 ± 24	1571 ± 99

according to their probability density functions, taking correlations into account. For normalization uncertainties, log-normal probability density functions are used as priors. For shape uncertainties, polynomial interpolation is used to derive continuous prior distributions from the nominal and varied m_T shape templates. The expected event yields after a background-only fit to the data and the observed yields are summarized in Table 3.

The distributions of m_T after a background-only fit to the data are shown in Fig. 3 for both categories in the τ_h + jets final state, in Fig. 4 for two categories with high signal sensitivity in the ℓ + τ_h final state, and in Fig. 5 for two high-sensitivity categories in the ℓ + no τ_h final state. No significant excess is observed in any of the categories, and the result of the simultaneous fit is found to agree with the SM prediction.

The modified frequentist CL_s criterion [85, 86] based on the profile likelihood ratio test statistic [87] is applied to determine the 95% confidence level (CL) limit for the product of the $H^{\pm}$ production cross section and the branching fraction $\mathcal{B}(H^{\pm} \to \tau^{\pm}\nu_{\tau})$. The asymptotic approximation [88] is used throughout the analysis. Pseudo-experiments are performed for selected signal mass hypotheses to verify the validity of the asymptotic approximation. For the $H^{\pm}$ mass range up to 165 GeV, the limit on $\mathcal{B}(t \to bH^{\pm})\mathcal{B}(H^{\pm} \to \tau^{\pm}\nu_{\tau})$ is calculated, scaling down the $t\bar{t}$ background component consistently with the $\mathcal{B}(t \to bH^{\pm})$ signal hypothesis, and the result is interpreted as a limit on $\sigma_{H^{\pm}}\mathcal{B}(H^{\pm} \to \tau^{\pm}\nu_{\tau})$ by assuming $\sigma_{H^{\pm}} = 2\sigma_{t\bar{t}}\mathcal{B}(t \to bH^{\pm})(1 - \mathcal{B}(t \to bH^{\pm}))$, where the $t\bar{t}$ production cross section $\sigma_{t\bar{t}}$ is assumed unmodified by the presence of $H^{\pm}$ and the value of 831.76 pb is used [55, 56]. For the $H^{\pm}$ mass range from 170 GeV to 3 TeV, the limit on $\sigma_{H^{\pm}}\mathcal{B}(H^{\pm} \to \tau^{\pm}\nu_{\tau})$ is calculated without assuming a specific production mode.

The model-independent upper limit with all final states and categories combined is shown on the left side of Fig. 6. The numerical values are listed in Table 4. The observed limit ranges from 6 pb at 80 GeV to 5 fb at 3 TeV. For the light $H^{\pm}$ mass range of 80–160 GeV, the limit corresponds to $\mathcal{B}(t \to bH^{\pm})\mathcal{B}(H^{\pm} \to \tau^{\pm}\nu_{\tau})$ values between 0.36% (at 80 GeV) and 0.08% (at 160 GeV). In the light $H^{\pm}$ mass range, this is the most stringent limit on $\mathcal{B}(t \to bH^{\pm})\mathcal{B}(H^{\pm} \to \tau^{\pm}\nu_{\tau})$ to date set by the CMS Collaboration, with a factor of 1.5–3.0 improvement with respect to Ref. [28], depending on $m_{H^{\pm}}$. In the intermediate mass range of 165–175 GeV, this is the first limit on

$\sigma_{H^\pm}\mathcal{B}(H^\pm \to \tau^\pm\nu_\tau)$ set by the CMS Collaboration. The drop in the expected and observed limits in the intermediate region is not predicted from theory [20] but is rather an experimental feature explained by the fact that in this region LO signal samples are used instead of NLO. This dip is mitigated but not completely cancelled by the LO-to-NLO corrections extrapolated from the surrounding mass regions. In the heavy mass range from 180 GeV, this result extends the search region up to $m_{H^\pm} = 3$ TeV, compared to 600 GeV in Ref. [28].

In the light and intermediate $H^\pm$ mass regions all three final states contribute significantly to the sensitivity, and the combined limits are on average ≈40% lower compared to the τ_h + jets final state alone. In the heavy $H^\pm$ mass region, the sensitivity of the leptonic final states decreases, and the τ_h + jets final state starts to dominate the limit as $m_{H^\pm}$ increases. Above $m_{H^\pm} = 500$ GeV the combined limit is solely driven by the τ_h + jets final state.

The limit is interpreted in the MSSM $m_h^{\text{mod-}}$ benchmark scenario [89] by comparing the observed limit on the $H^\pm$ cross section to the theoretical cross sections predicted in this scenario [20, 90–94]. The MSSM $m_h^{\text{mod-}}$ scenario is specified using low-energy MSSM parameters and is designed to give a mass of approximately 125 GeV for the light CP-even Higgs boson over a wide region of the parameter space. The limit for the MSSM $m_h^{\text{mod-}}$ scenario in the $m_{H^\pm}$–tan β plane is shown on the right side of Fig. 6. Based on the observed limit, all values of the parameter tan β from 1 to 60 are excluded for $m_{H^\pm}$ values up to 160 GeV. The limit extends to $m_{H^\pm} = 500$ GeV. For $m_{H^\pm} = 200$ (400) GeV, the observed limit excludes all tan β values above 26 (40), compared to 45 (56) excluded in Ref. [28].

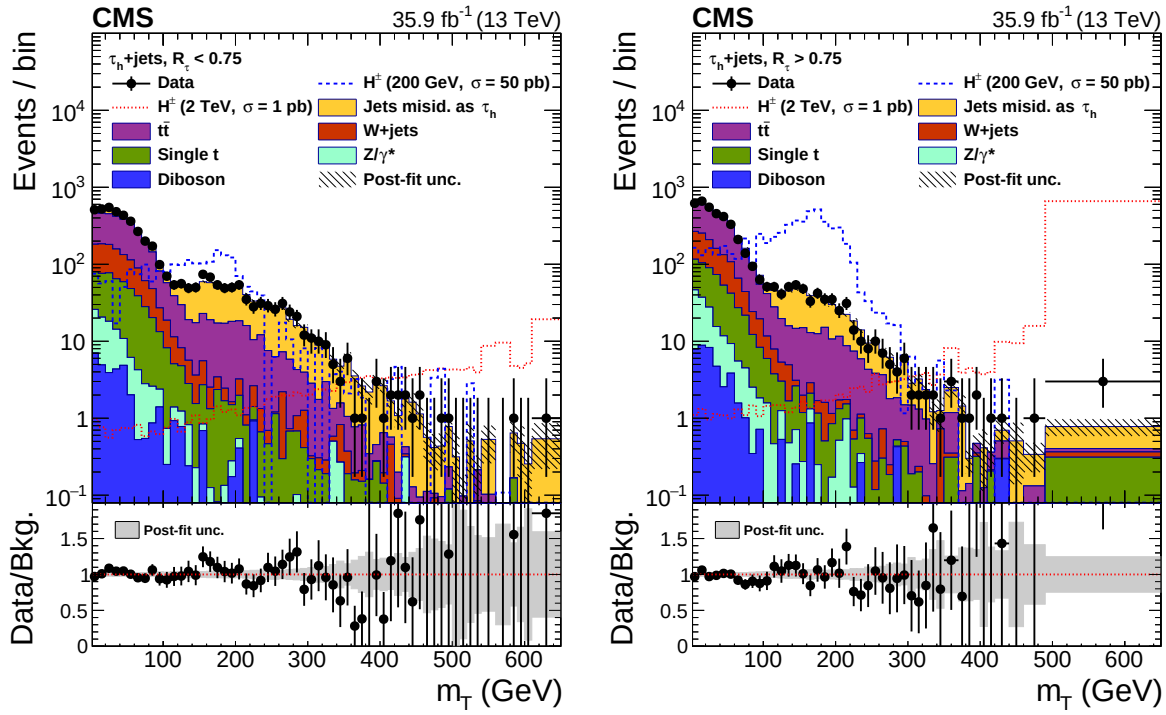

Figure 3: The transverse mass distributions in the τ_h + jets final state after a background-only fit to the data. Left: category defined by $R_\tau < 0.75$. Transverse mass values up to 5 TeV are considered in the fit, but the last bins with $m_T > 650$ GeV do not contain any observed events. Right: category defined by $R_\tau > 0.75$. The last bin shown extends to 5 TeV.

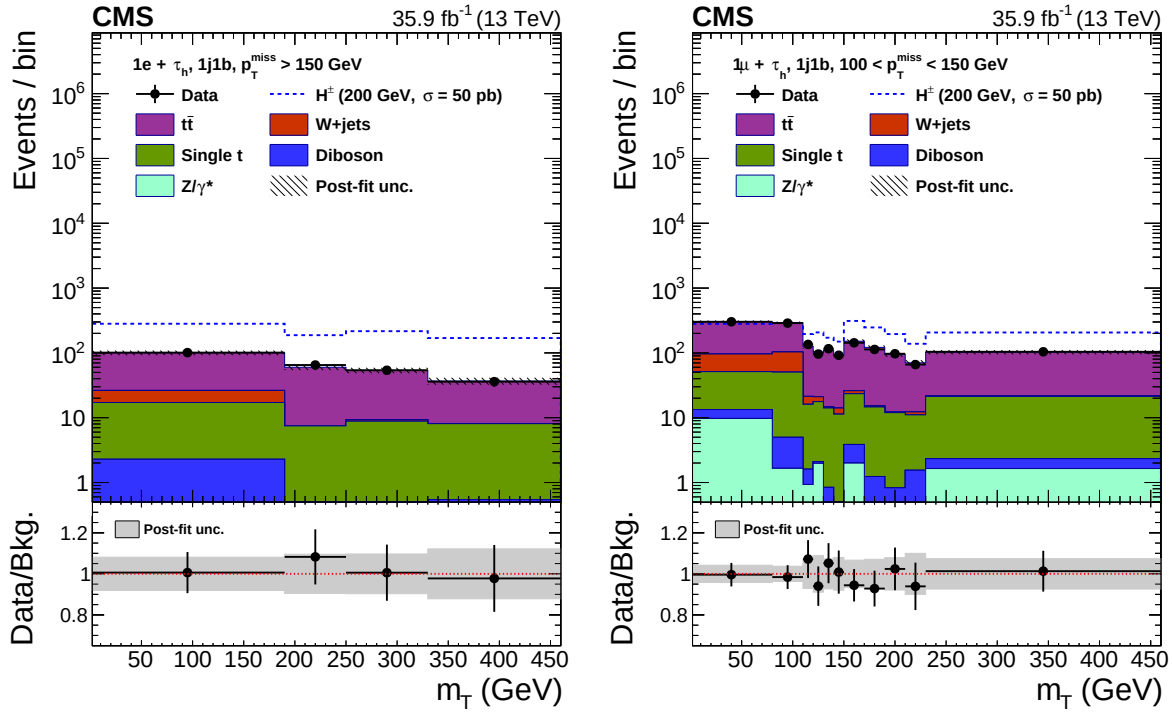

Figure 4: The transverse mass distributions for two ℓ + τ_h categories with high signal sensitivity after a background-only fit to the data. Left: category with one electron, one τ_h, one jet identified as a b jet, and $p_T^{miss} > 150$ GeV. Right: category with one muon, one τ_h, one jet identified as a b jet and $100 < p_T^{miss} < 150$ GeV. In both categories, the last bin shown extends to 5 TeV.

Table 4: The expected and observed 95% CL exclusion limits on $\sigma_{H^\pm}\mathcal{B}(H^\pm \to \tau^\pm\nu_\tau)$ for the $H^\pm$ mass range from 80 GeV to 3 TeV. The ± 1 s.d. (± 2 s.d.) refers to one (two) standard deviations from the expected limit.

$m_{H^\pm}$	Expected limit (pb)					Observed
(GeV)	-2 s.d.	-1 s.d.	median	+1 s.d.	+2 s.d.	limit (pb)
80	3.17	4.25	5.87	8.15	10.89	5.97
90	3.05	4.08	5.69	7.96	10.75	4.59
100	2.67	3.56	4.94	6.90	9.26	3.24
120	2.04	2.72	3.78	5.29	7.12	2.55
140	1.41	1.87	2.61	3.63	4.88	2.22
150	1.19	1.58	2.20	3.07	4.14	1.63
155	1.06	1.41	1.95	2.71	3.64	1.48
160	1.05	1.39	1.93	2.69	3.61	1.31
165	0.76	1.02	1.45	2.67	2.86	1.01
170	0.40	0.54	0.77	1.12	1.59	0.57
175	0.37	0.50	0.71	1.03	1.45	0.52
180	0.44	0.60	0.83	1.18	1.59	0.85
200	0.30	0.41	0.57	0.80	1.09	0.65
220	0.22	0.30	0.41	0.58	0.80	0.47
250	0.15	0.21	0.29	0.41	0.56	0.31
300	0.08	0.11	0.15	0.22	0.30	0.14
400	0.032	0.043	0.062	0.090	0.125	0.078
500	0.016	0.022	0.031	0.046	0.067	0.048
750	0.0035	0.0050	0.0077	0.012	0.019	0.014
800	0.0029	0.0041	0.0064	0.0102	0.0157	0.0107
1000	0.0020	0.0030	0.0047	0.0077	0.0121	0.0085
2000	0.0009	0.0014	0.0025	0.0044	0.0074	0.0050
2500	0.0007	0.0012	0.0022	0.0042	0.0068	0.0047
3000	0.0007	0.0012	0.0022	0.0043	0.0067	0.0048

9 Summary

A search is presented for charged Higgs bosons decaying as $H^{\pm} \to \tau^{\pm}\nu_{\tau}$, using events recorded by the CMS experiment in 2016 at a center-of-mass energy of 13 TeV. Transverse mass distributions are reconstructed in hadronic and leptonic final states and are found to agree with the standard model expectation. Upper limits for the product of the $H^{\pm}$ production cross section and the branching fraction to $\tau^{\pm}\nu_{\tau}$ are set at 95% confidence level for an $H^{\pm}$ mass ranging from 80 GeV to 3 TeV, including the range close to the top quark mass. The observed limit ranges from 6 pb at 80 GeV to 5 fb at 3 TeV. The results are interpreted as constraints in the parameter space of the minimal supersymmetric standard model $m_{h}^{\text{mod-}}$ benchmark scenario. In this scenario, all $\tan\beta$ values from 1 to 60 are excluded for charged Higgs boson masses up to 160 GeV.

Acknowledgments

We congratulate our colleagues in the CERN accelerator departments for the excellent performance of the LHC and thank the technical and administrative staffs at CERN and at other CMS institutes for their contributions to the success of the CMS effort. In addition, we gratefully acknowledge the computing centers and personnel of the Worldwide LHC Computing Grid for delivering so effectively the computing infrastructure essential to our analyses. Finally, we acknowledge the enduring support for the construction and operation of the LHC and the CMS detector provided by the following funding agencies: BMBWF and FWF (Austria); FNRS and FWO (Belgium); CNPq, CAPES, FAPERJ, FAPERGS, and FAPESP (Brazil); MES (Bulgaria); CERN; CAS, MoST, and NSFC (China); COLCIENCIAS (Colombia); MSES and CSF (Croa-

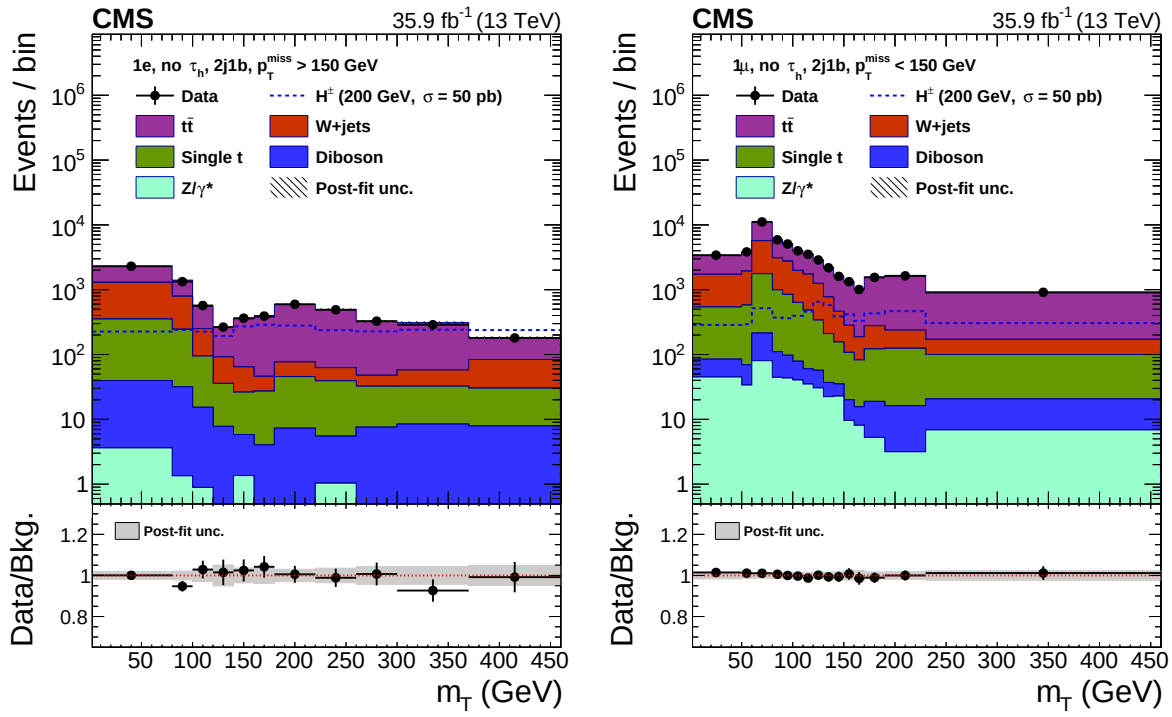

Figure 5: The m_{T} distributions for two ℓ + no τ_{h} categories with high signal sensitivity after a background-only fit to the data. Left: category with one electron, no τ_{h}, two jets (one identified as a b jet), and $p_{\mathrm{T}}^{\mathrm{miss}} > 150$ GeV. Right: category with one muon, no τ_{h}, two jets (one identified as a b jet) and $p_{\mathrm{T}}^{\mathrm{miss}} < 150$ GeV. In both categories, the last bin shown extends to 5 TeV.

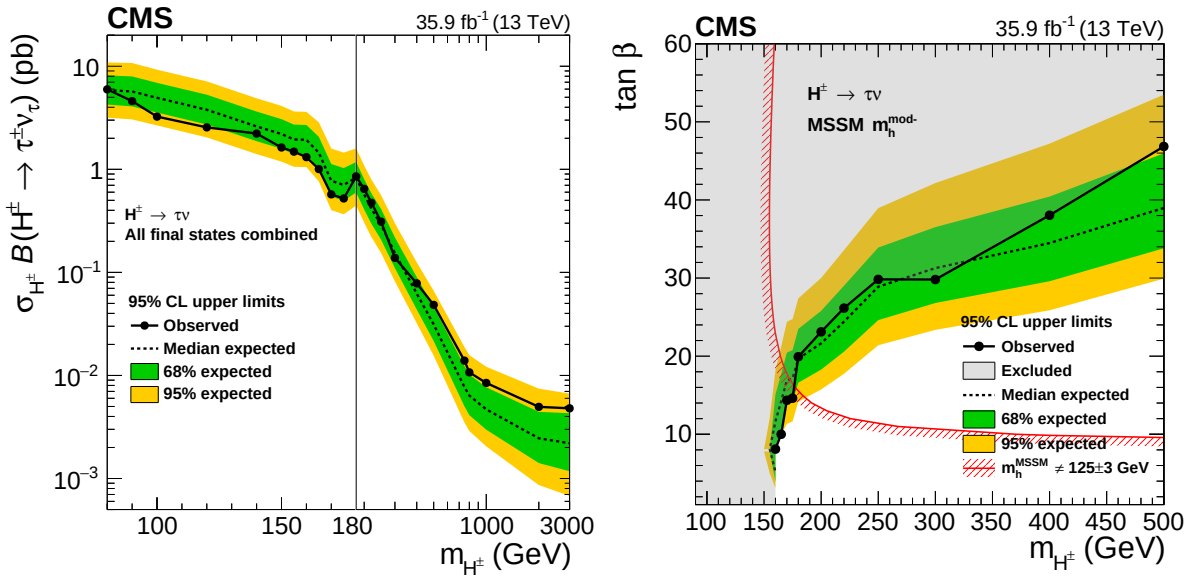

Figure 6: The observed 95% CL exclusion limits on $\sigma_{H^\pm}\mathcal{B}(H^\pm \to \tau^\pm\nu_\tau)$ (solid black points), compared to the expected limit assuming only standard model processes (dashed line) for the $H^\pm$ mass range from 80 GeV to 3 TeV (left), and the same limit interpreted in the $m_h^{\text{mod-}}$ benchmark scenario (right). The green (yellow) bands represent one (two) standard deviations from the expected limit. On the left, the horizontal axis is linear from 80 to 180 GeV and logarithmic for larger $m_{H^\pm}$ values. On the right, the region below the red line is excluded assuming that the observed neutral Higgs boson is the light CP-even 2HDM Higgs boson with a mass of 125 ± 3 GeV, where the uncertainty is the theoretical uncertainty in the mass calculation.

tia); RPF (Cyprus); SENESCYT (Ecuador); MoER, ERC IUT, and ERDF (Estonia); Academy of Finland, MEC, and HIP (Finland); CEA and CNRS/IN2P3 (France); BMBF, DFG, and HGF (Germany); GSRT (Greece); NKFIA (Hungary); DAE and DST (India); IPM (Iran); SFI (Ireland); INFN (Italy); MSIP and NRF (Republic of Korea); MES (Latvia); LAS (Lithuania); MOE and UM (Malaysia); BUAP, CINVESTAV, CONACYT, LNS, SEP, and UASLP-FAI (Mexico); MOS (Montenegro); MBIE (New Zealand); PAEC (Pakistan); MSHE and NSC (Poland); FCT (Portugal); JINR (Dubna); MON, RosAtom, RAS, RFBR, and NRC KI (Russia); MESTD (Serbia); SEIDI, CPAN, PCTI, and FEDER (Spain); MOSTR (Sri Lanka); Swiss Funding Agencies (Switzerland); MST (Taipei); ThEPCenter, IPST, STAR, and NSTDA (Thailand); TUBITAK and TAEK (Turkey); NASU and SFFR (Ukraine); STFC (United Kingdom); DOE and NSF (USA).

Individuals have received support from the Marie-Curie program and the European Research Council and Horizon 2020 Grant, contract No. 675440 (European Union); the Leventis Foundation; the A. P. Sloan Foundation; the Alexander von Humboldt Foundation; the Belgian Federal Science Policy Office; the Fonds pour la Formation à la Recherche dans l'Industrie et dans l'Agriculture (FRIA-Belgium); the Agentschap voor Innovatie door Wetenschap en Technologie (IWT-Belgium); the F.R.S.-FNRS and FWO (Belgium) under the "Excellence of Science - EOS" - be.h project n. 30820817; the Ministry of Education, Youth and Sports (MEYS) of the Czech Republic; the Lendület ("Momentum") Program and the János Bolyai Research Scholarship of the Hungarian Academy of Sciences, the New National Excellence Program ÚNKP, the NKFIA research grants 123842, 123959, 124845, 124850 and 125105 (Hungary); the Council of Science and Industrial Research, India; the HOMING PLUS program of the Foundation for Polish Science, cofinanced from European Union, Regional Development Fund, the Mobility Plus program of the Ministry of Science and Higher Education, the National Science Center (Poland), contracts Harmonia 2014/14/M/ST2/00428, Opus 2014/13/B/ST2/02543, 2014/15/B/ST2/03998, and

2015/19/B/ST2/02861, Sonata-bis 2012/07/E/ST2/01406; the National Priorities Research Program by Qatar National Research Fund; the Programa Estatal de Fomento de la Investigación Científica y Técnica de Excelencia María de Maeztu, grant MDM-2015-0509 and the Programa Severo Ochoa del Principado de Asturias; the Thalis and Aristeia programs cofinanced by EU-ESF and the Greek NSRF; the Rachadapisek Sompot Fund for Postdoctoral Fellowship, Chulalongkorn University and the Chulalongkorn Academic into Its 2nd Century Project Advancement Project (Thailand); the Welch Foundation, contract C-1845; and the Weston Havens Foundation (USA).

References

[1] ATLAS Collaboration, "Observation of a new particle in the search for the standard model Higgs boson with the ATLAS detector at the LHC", *Phys. Lett. B* **716** (2012) 1, doi:10.1016/j.physletb.2012.08.020, arXiv:1207.7214.

[2] CMS Collaboration, "Observation of a new boson at a mass of 125 GeV with the CMS experiment at the LHC", *Phys. Lett. B* **716** (2012) 30, doi:10.1016/j.physletb.2012.08.021, arXiv:1207.7235.

[3] CMS Collaboration, "Observation of a new boson with mass near 125 GeV in pp collisions at $\sqrt{s}$ = 7 and 8 TeV", *JHEP* **06** (2013) 081, doi:10.1007/JHEP06(2013)081, arXiv:1303.4571.

[4] P. W. Higgs, "Broken symmetries, massless particles and gauge fields", *Phys. Lett.* **12** (1964) 132, doi:10.1016/0031-9163(64)91136-9.

[5] P. W. Higgs, "Broken symmetries and the masses of gauge bosons", *Phys. Rev. Lett.* **13** (1964) 508, doi:10.1103/PhysRevLett.13.508.

[6] G. S. Guralnik, C. R. Hagen, and T. W. B. Kibble, "Global conservation laws and massless particles", *Phys. Rev. Lett.* **13** (1964) 585, doi:10.1103/PhysRevLett.13.585.

[7] P. W. Higgs, "Spontaneous symmetry breakdown without massless bosons", *Phys. Rev.* **145** (1966) 1156, doi:10.1103/PhysRev.145.1156.

[8] T. W. B. Kibble, "Symmetry breaking in non-Abelian gauge theories", *Phys. Rev.* **155** (1967) 1554, doi:10.1103/PhysRev.155.1554.

[9] F. Englert and R. Brout, "Broken symmetry and the mass of gauge vector mesons", *Phys. Rev. Lett.* **13** (1964) 321, doi:10.1103/PhysRevLett.13.321.

[10] CMS Collaboration, "Constraints on the spin-parity and anomalous HVV couplings of the Higgs boson in proton collisions at 7 and 8 TeV", *Phys. Rev. D* **92** (2015) 012004, doi:10.1103/PhysRevD.92.012004, arXiv:1411.3441.

[11] ATLAS and CMS Collaborations, "Combined measurement of the Higgs boson mass in pp collisions at $\sqrt{s} = 7$ and 8 TeV with the ATLAS and CMS experiments", *Phys. Rev. Lett.* **114** (2015) 191803, doi:10.1103/PhysRevLett.114.191803, arXiv:1503.07589.

[12] ATLAS Collaboration, "Study of the spin and parity of the Higgs boson in diboson decays with the ATLAS detector", *Eur. Phys. J. C* **75** (2015) 476, doi:10.1140/epjc/s10052-015-3685-1, arXiv:1506.05669. [Erratum: doi:10.1140/epjc/s10052-016-3934-y].

[13] ATLAS and CMS Collaborations, "Measurements of the Higgs boson production and decay rates and constraints on its couplings from a combined ATLAS and CMS analysis of the LHC pp collision data at $\sqrt{s} = 7$ and 8 TeV", *JHEP* **08** (2016) 045, doi:10.1007/JHEP08(2016)045, arXiv:1606.02266.

[14] CMS Collaboration, "Measurements of properties of the Higgs boson decaying into the four-lepton final state in pp collisions at $\sqrt{s} = 13$ TeV", *JHEP* **11** (2017) 047, doi:10.1007/JHEP11(2017)047, arXiv:1706.09936.

[15] G. C. Branco et al., "Theory and phenomenology of two-Higgs-doublet models", *Phys. Rept.* **516** (2012) 1, doi:10.1016/j.physrep.2012.02.002, arXiv:1106.0034.

[16] A. Djouadi, "The anatomy of electro-weak symmetry breaking. II. the Higgs bosons in the minimal supersymmetric model", *Phys. Rept.* **459** (2008) 1, doi:10.1016/j.physrep.2007.10.005, arXiv:hep-ph/0503173.

[17] G. Senjanovic and R. N. Mohapatra, "Exact left-right symmetry and spontaneous violation of parity", *Phys. Rev. D* **12** (1975) 1502, doi:10.1103/PhysRevD.12.1502.

[18] J. F. Gunion, R. Vega, and J. Wudka, "Higgs triplets in the standard model", *Phys. Rev. D* **42** (1990) 1673, doi:10.1103/PhysRevD.42.1673.

[19] H. Georgi and M. Machacek, "Doubly charged Higgs bosons", *Nucl. Phys. B* **262** (1985) 463, doi:10.1016/0550-3213(85)90325-6.

[20] C. Degrande et al., "Accurate predictions for charged Higgs production: Closing the $m_{h^\pm} \sim m_t$ window", *Phys. Lett. B* **772** (2017) 87, doi:10.1016/j.physletb.2017.06.037, arXiv:1607.05291.

[21] ALEPH, DELPHI, L3, OPAL and LEP Collaborations, "Search for charged Higgs bosons: combined results using LEP data", *Eur. Phys. J. C* **73** (2013) 2463, doi:10.1140/epjc/s10052-013-2463-1, arXiv:1301.6065.

[22] CDF Collaboration, "Search for Higgs bosons predicted in two-Higgs-doublet models via decays to tau lepton pairs in 1.96 TeV $p\bar{p}$ collisions", *Phys. Rev. Lett.* **103** (2009) 201801, doi:10.1103/PhysRevLett.103.201801, arXiv:0906.1014.

[23] D0 Collaboration, "Search for Higgs bosons of the minimal supersymmetric standard model in $p\bar{p}$ collisions at $\sqrt{s} = 1.96$ TeV", *Phys. Lett. B* **710** (2012) 569, doi:10.1016/j.physletb.2012.03.021, arXiv:1112.5431.

[24] ATLAS Collaboration, "Search for charged Higgs bosons decaying via $H^+ \to \tau\nu$ in top quark pair events using pp collision data at $\sqrt{s} = 7$ TeV with the ATLAS detector", *JHEP* **06** (2012) 039, doi:10.1007/JHEP06(2012)039, arXiv:1204.2760.

[25] CMS Collaboration, "Search for a light charged Higgs boson in top quark decays in pp collisions at $\sqrt{s} = 7$ TeV", *JHEP* **07** (2012) 143, doi:10.1007/JHEP07(2012)143, arXiv:1205.5736.

[26] ATLAS Collaboration, "Search for charged Higgs bosons through the violation of lepton universality in $t\bar{t}$ events using pp collision data at $\sqrt{s} = 7$ TeV with the ATLAS experiment", *JHEP* **03** (2013) 076, doi:10.1007/JHEP03(2013)076, arXiv:1212.3572.

[27] ATLAS Collaboration, "Search for charged Higgs bosons decaying via $H^{\pm} \to \tau^{\pm}\nu$ in fully hadronic final states using pp collision data at $\sqrt{s} = 8$ TeV with the ATLAS detector", *JHEP* **03** (2015) 088, doi:10.1007/JHEP03(2015)088, arXiv:1412.6663.

[28] CMS Collaboration, "Search for a charged Higgs boson in pp collisions at $\sqrt{s} = 8$ TeV", *JHEP* **11** (2015) 018, doi:10.1007/JHEP11(2015)018, arXiv:1508.07774.

[29] ATLAS Collaboration, "Search for charged Higgs bosons produced in association with a top quark and decaying via $H^{\pm} \to \tau\nu$ using pp collision data recorded at $\sqrt{s} = 13$ TeV by the ATLAS detector", *Phys. Lett. B* **759** (2016) 555, doi:10.1016/j.physletb.2016.06.017, arXiv:1603.09203.

[30] ATLAS Collaboration, "Search for charged Higgs bosons decaying via $H^{\pm} \to \tau^{\pm}\nu_{\tau}$ in the τ+jets and τ+lepton final states with 36 fb^{-1} of pp collision data recorded at $\sqrt{s} = 13$ TeV with the ATLAS experiment", *JHEP* **09** (2018) 139, doi:10.1007/JHEP09(2018)139, arXiv:1807.07915.

[31] ATLAS Collaboration, "Search for charged Higgs bosons in the $H^{\pm} \to tb$ decay channel in pp collisions at $\sqrt{s} = 8$ TeV using the ATLAS detector", *JHEP* **03** (2016) 127, doi:10.1007/JHEP03(2016)127, arXiv:1512.03704.

[32] ATLAS Collaboration, "Search for charged Higgs bosons decaying into top and bottom quarks at $\sqrt{s}$ = 13 TeV with the ATLAS detector", *JHEP* **11** (2018) 085, doi:10.1007/JHEP11(2018)085, arXiv:1808.03599.

[33] ATLAS Collaboration, "Search for a light charged Higgs boson in the decay channel $H^{+} \to c\bar{s}$ in $t\bar{t}$ events using pp collisions at $\sqrt{s}$ = 7 TeV with the ATLAS detector", *Eur. Phys. J. C* **73** (2013) 2465, doi:10.1140/epjc/s10052-013-2465-z, arXiv:1302.3694.

[34] CMS Collaboration, "Search for a light charged Higgs boson decaying to $c\bar{s}$ in pp collisions at $\sqrt{s} = 8$ TeV", *JHEP* **12** (2015) 178, doi:10.1007/JHEP12(2015)178, arXiv:1510.04252.

[35] CMS Collaboration, "Search for a charged Higgs boson decaying to charm and bottom quarks in proton-proton collisions at $\sqrt{s} = 8$ TeV", *JHEP* **11** (2018) 115, doi:10.1007/JHEP11(2018)115, arXiv:1808.06575.

[36] ATLAS Collaboration, "Search for a charged Higgs boson produced in the vector-boson fusion mode with decay $H^{\pm} \to W^{\pm}Z$ using pp collisions at $\sqrt{s} = 8$ TeV with the ATLAS experiment", *Phys. Rev. Lett.* **114** (2015) 231801, doi:10.1103/PhysRevLett.114.231801, arXiv:1503.04233.

[37] CMS Collaboration, "Search for charged Higgs bosons produced via vector boson fusion and decaying into a pair of W and Z bosons using pp collisions at $\sqrt{s} = 13$ TeV", *Phys. Rev. Lett.* **119** (2017) 141802, doi:10.1103/PhysRevLett.119.141802, arXiv:1705.02942.

[38] ATLAS Collaboration, "Search for additional heavy neutral Higgs and gauge bosons in the ditau final state produced in 36 fb^{-1} of pp collisions at $\sqrt{s} = 13$ TeV with the ATLAS detector", *JHEP* **01** (2018) 055, doi:10.1007/JHEP01(2018)055, arXiv:1709.07242.

[39] CMS Collaboration, "Search for additional neutral MSSM Higgs bosons in the $\tau\tau$ final state in proton-proton collisions at $\sqrt{s} = 13$ TeV", *JHEP* **09** (2018) 007, doi:10.1007/JHEP09(2018)007, arXiv:1803.06553.

[40] CMS Collaboration, "Search for beyond the standard model Higgs bosons decaying into a $\mathrm{b\bar{b}}$ pair in pp collisions at $\sqrt{s} = 13$ TeV", *JHEP* **08** (2018) 113, doi:10.1007/JHEP08(2018)113, arXiv:1805.12191.

[41] A. Arbey, F. Mahmoudi, O. Stal, and T. Stefaniak, "Status of the charged Higgs boson in two Higgs doublet models", *Eur. Phys. J. C* **78** (2018) 182, doi:10.1140/epjc/s10052-018-5651-1, arXiv:1706.07414.

[42] CMS Collaboration, "The CMS trigger system", *JINST* **12** (2017) P01020, doi:10.1088/1748-0221/12/01/P01020, arXiv:1609.02366.

[43] CMS Collaboration, "The CMS experiment at the CERN LHC", *JINST* **3** (2008) S08004, doi:10.1088/1748-0221/3/08/S08004.

[44] J. Alwall et al., "The automated computation of tree-level and next-to-leading order differential cross sections, and their matching to parton shower simulations", *JHEP* **07** (2014) 079, doi:10.1007/JHEP07(2014)079, arXiv:1405.0301.

[45] P. Artoisenet, R. Frederix, O. Mattelaer, and R. Rietkerk, "Automatic spin-entangled decays of heavy resonances in Monte Carlo simulations", *JHEP* **03** (2013) 015, doi:10.1007/JHEP03(2013)015, arXiv:1212.3460.

[46] P. Nason, "A new method for combining NLO QCD with shower Monte Carlo algorithms", *JHEP* **11** (2004) 040, doi:10.1088/1126-6708/2004/11/040, arXiv:hep-ph/0409146.

[47] S. Frixione, P. Nason, and C. Oleari, "Matching NLO QCD computations with parton shower simulations: the POWHEG method", *JHEP* **11** (2007) 070, doi:10.1088/1126-6708/2007/11/070, arXiv:0709.2092.

[48] S. Alioli, P. Nason, C. Oleari, and E. Re, "A general framework for implementing NLO calculations in shower Monte Carlo programs: the POWHEG BOX", *JHEP* **06** (2010) 043, doi:10.1007/JHEP06(2010)043, arXiv:1002.2581.

[49] T. Ježo et al., "An NLO+PS generator for $\mathrm{t\bar{t}}$ and Wt production and decay including non-resonant and interference effects", *Eur. Phys. J. C* **76** (2016) 691, doi:10.1140/epjc/s10052-016-4538-2, arXiv:1607.04538.

[50] S. Frixione, P. Nason, and G. Ridolfi, "A positive-weight next-to-leading-order Monte Carlo for heavy flavour hadroproduction", *JHEP* **09** (2007) 126, doi:10.1088/1126-6708/2007/09/126, arXiv:0707.3088.

[51] R. Frederix and S. Frixione, "Merging meets matching in MC@NLO", *JHEP* **12** (2012) 061, doi:10.1007/JHEP12(2012)061, arXiv:1209.6215.

[52] S. Alioli, P. Nason, C. Oleari, and E. Re, "NLO single-top production matched with shower in POWHEG: s- and t-channel contributions", *JHEP* **09** (2009) 111, doi:10.1007/JHEP02(2010)011, arXiv:0907.4076. [Erratum: doi:10.1088/1126-6708/2009/09/111].

[53] E. Re, "Single-top Wt-channel production matched with parton showers using the POWHEG method", *Eur. Phys. J. C* **71** (2011) 1547, doi:10.1140/epjc/s10052-011-1547-z, arXiv:1009.2450.

[54] J. Alwall et al., "Comparative study of various algorithms for the merging of parton showers and matrix elements in hadronic collisions", *Eur. Phys. J. C* **53** (2008) 473, doi:10.1140/epjc/s10052-007-0490-5, arXiv:0706.2569.

[55] M. Czakon and A. Mitov, "Top++: A program for the calculation of the top-pair cross-section at hadron colliders", *Comput. Phys. Commun.* **185** (2014) 2930, doi:10.1016/j.cpc.2014.06.021, arXiv:1112.5675.

[56] N. Kidonakis, "Top quark production", in *Proceedings, Helmholtz International Summer School on Physics of Heavy Quarks and Hadrons (HQ 2013)*, p. 139. 2014. arXiv:1311.0283. doi:10.3204/DESY-PROC-2013-03/Kidonakis.

[57] P. Kant et al., "HatHor for single top-quark production: Updated predictions and uncertainty estimates for single top-quark production in hadronic collisions", *Comput. Phys. Commun.* **191** (2015) 74, doi:10.1016/j.cpc.2015.02.001, arXiv:1406.4403.

[58] K. Melnikov and F. Petriello, "Electroweak gauge boson production at hadron colliders through $O(\alpha_s^2)$", *Phys. Rev. D* **74** (2006) 114017, doi:10.1103/PhysRevD.74.114017, arXiv:hep-ph/0609070.

[59] J. M. Campbell, R. K. Ellis, and C. Williams, "Vector boson pair production at the LHC", *JHEP* **07** (2011) 018, doi:10.1007/JHEP07(2011)018, arXiv:1105.0020.

[60] NNPDF Collaboration, "Unbiased global determination of parton distributions and their uncertainties at NNLO and at LO", *Nucl. Phys. B* **855** (2012) 153, doi:10.1016/j.nuclphysb.2011.09.024, arXiv:1107.2652.

[61] CMS Collaboration, "Event generator tunes obtained from underlying event and multiparton scattering measurements", *Eur. Phys. J. C* **76** (2016) 155, doi:10.1140/epjc/s10052-016-3988-x, arXiv:1512.00815.

[62] CMS Collaboration, "Investigations of the impact of the parton shower tuning in PYTHIA 8 in the modelling of $\mathrm{t\bar{t}}$ at $\sqrt{s} = 8$ and 13 TeV", CMS Physics Analysis Summary CMS-PAS-TOP-16-021, 2016.

[63] GEANT4 Collaboration, "GEANT4—a simulation toolkit", *Nucl. Instrum. Meth. A* **506** (2003) 250, doi:10.1016/S0168-9002(03)01368-8.

[64] CMS Collaboration, "Particle-flow reconstruction and global event description with the CMS detector", *JINST* **12** (2017) P10003, doi:10.1088/1748-0221/12/10/P10003, arXiv:1706.04965.

[65] K. Rose, "Deterministic annealing for clustering, compression, classification, regression, and related optimization problems", *Proceedings of the IEEE* **86** (1998) 2210, doi:10.1109/5.726788.

[66] M. Cacciari, G. P. Salam, and G. Soyez, "The anti-k_{T} jet clustering algorithm", *JHEP* **04** (2008) 063, doi:10.1088/1126-6708/2008/04/063, arXiv:0802.1189.

[67] M. Cacciari, G. P. Salam, and G. Soyez, "FastJet user manual", *Eur. Phys. J. C* **72** (2012) 1896, doi:10.1140/epjc/s10052-012-1896-2, arXiv:1111.6097.

[68] CMS Collaboration, "Performance of electron reconstruction and selection with the CMS detector in proton-proton collisions at $\sqrt{s} = 8$ TeV", *JINST* **10** (2015) P06005, doi:10.1088/1748-0221/10/06/P06005, arXiv:1502.02701.

[69] H. Voss, A. Höcker, J. Stelzer, and F. Tegenfeldt, "TMVA, the toolkit for multivariate data analysis with ROOT", in *XIth International Workshop on Advanced Computing and Analysis Techniques in Physics Research (ACAT)*, p. 40. 2007. arXiv:physics/0703039.

[70] CMS Collaboration, "Performance of the CMS muon detector and muon reconstruction with proton-proton collisions at $\sqrt{s} = 13$ TeV", *JINST* **13** (2018) P06015, doi:10.1088/1748-0221/13/06/P06015, arXiv:1804.04528.

[71] CMS Collaboration, "Jet energy scale and resolution in the CMS experiment in pp collisions at 8 TeV", *JINST* **12** (2017) P02014, doi:10.1088/1748-0221/12/02/P02014, arXiv:1607.03663.

[72] CMS Collaboration, "Jet algorithms performance in 13 TeV data", CMS Physics Analysis Summary CMS-PAS-JME-16-003, 2017.

[73] CMS Collaboration, "Identification of b-quark jets with the CMS experiment", *JINST* **8** (2013) P04013, doi:10.1088/1748-0221/8/04/P04013, arXiv:1211.4462.

[74] CMS Collaboration, "Identification of heavy-flavour jets with the CMS detector in pp collisions at 13 TeV", *JINST* **13** (2018) P05011, doi:10.1088/1748-0221/13/05/P05011, arXiv:1712.07158.

[75] CMS Collaboration, "Reconstruction and identification of τ lepton decays to hadrons and ν_τ at CMS", *JINST* **11** (2016) P01019, doi:10.1088/1748-0221/11/01/P01019, arXiv:1510.07488.

[76] CMS Collaboration, "Performance of reconstruction and identification of τ leptons decaying to hadrons and ν_τ in pp collisions at $\sqrt{s} = 13$ TeV", *JINST* **13** (2018) P10005, doi:10.1088/1748-0221/13/10/P10005, arXiv:1809.02816.

[77] CMS Collaboration, "Performance of missing transverse momentum in pp collisions at $\sqrt{s} = 13$ TeV using the CMS detector", CMS Physics Analysis Summary CMS-PAS-JME-17-001, 2018.

[78] CMS Collaboration, "Performance of CMS muon reconstruction in pp collision events at $\sqrt{s} = 7$ TeV", *JINST* **7** (2012) P10002, doi:10.1088/1748-0221/7/10/P10002, arXiv:1206.4071.

[79] D. P. Roy, "The hadronic tau decay signature of a heavy charged Higgs boson at LHC", *Phys. Lett. B* **459** (1999) 607, doi:10.1016/S0370-2693(99)00724-8, arXiv:hep-ph/9905542.

[80] ATLAS Collaboration, "Measurement of the inelastic proton-proton cross section at $\sqrt{s} = 13$ TeV with the ATLAS detector at the LHC", *Phys. Rev. Lett.* **117** (2016) 182002, doi:10.1103/PhysRevLett.117.182002, arXiv:1606.02625.

[81] CMS Collaboration, "CMS luminosity measurements for the 2016 data taking period", CMS Physics Analysis Summary CMS-PAS-LUM-17-001, 2017.

[82] J. Butterworth et al., "PDF4LHC recommendations for LHC Run II", *J. Phys. G* **43** (2016) 023001, doi:10.1088/0954-3899/43/2/023001, arXiv:1510.03865.

[83] P. Skands, S. Carrazza, and J. Rojo, "Tuning PYTHIA 8.1: the Monash 2013 tune", *Eur. Phys. J. C* **74** (2014) 3024, doi:10.1140/epjc/s10052-014-3024-y, arXiv:1404.5630.

[84] R. J. Barlow and C. Beeston, "Fitting using finite Monte Carlo samples", *Comput. Phys. Commun.* **77** (1993) 219, doi:10.1016/0010-4655(93)90005-W.

[85] T. Junk, "Confidence level computation for combining searches with small statistics", *Nucl. Instrum. Meth. A* **434** (1999) 435, doi:10.1016/S0168-9002(99)00498-2, arXiv:hep-ex/9902006.

[86] A. L. Read, "Presentation of search results: The CL_s technique", *J. Phys. G* **28** (2002) 2693, doi:10.1088/0954-3899/28/10/313.

[87] ATLAS and CMS Collaborations, The LHC Higgs Combination Group, "Procedure for the LHC Higgs boson search combination in Summer 2011", Technical Report CMS-NOTE-2011-005, ATL-PHYS-PUB-2011-11, 2011.

[88] G. Cowan, K. Cranmer, E. Gross, and O. Vitells, "Asymptotic formulae for likelihood-based tests of new physics", *Eur. Phys. J. C* **71** (2011) 1554, doi:10.1140/epjc/s10052-011-1554-0, arXiv:1007.1727. [Erratum: doi:10.1140/epjc/s10052-013-2501-z].

[89] M. Carena et al., "MSSM Higgs boson searches at the LHC: Benchmark scenarios after the discovery of a Higgs-like particle", *Eur. Phys. J. C* **73** (2013) 2552, doi:10.1140/epjc/s10052-013-2552-1, arXiv:1302.7033.

[90] D. de Florian et al., "Handbook of LHC Higgs cross sections: 4. deciphering the nature of the Higgs sector", CERN Report CERN-2017-002-M, 2016. doi:10.23731/CYRM-2017-002, arXiv:1610.07922.

[91] M. Flechl et al., "Improved cross-section predictions for heavy charged Higgs boson production at the LHC", *Phys. Rev. D* **91** (2015) 075015, doi:10.1103/PhysRevD.91.075015, arXiv:1409.5615.

[92] C. Degrande, M. Ubiali, M. Wiesemann, and M. Zaro, "Heavy charged Higgs boson production at the LHC", *JHEP* **10** (2015) 145, doi:10.1007/JHEP10(2015)145, arXiv:1507.02549.

[93] S. Dittmaier, M. Kramer, M. Spira, and M. Walser, "Charged-Higgs-boson production at the LHC: NLO supersymmetric QCD corrections", *Phys. Rev. D* **83** (2011) 055005, doi:10.1103/PhysRevD.83.055005, arXiv:0906.2648.

[94] E. L. Berger, T. Han, J. Jiang, and T. Plehn, "Associated production of a top quark and a charged Higgs boson", *Phys. Rev. D* **71** (2005) 115012, doi:10.1103/PhysRevD.71.115012, arXiv:hep-ph/0312286.

A The CMS Collaboration

Yerevan Physics Institute, Yerevan, Armenia
A.M. Sirunyan, A. Tumasyan

Institut für Hochenergiephysik, Wien, Austria
W. Adam, F. Ambrogi, E. Asilar, T. Bergauer, J. Brandstetter, M. Dragicevic, J. Erö, A. Escalante Del Valle, M. Flechl, R. Frühwirth[1], V.M. Ghete, J. Hrubec, M. Jeitler[1], N. Krammer, I. Krätschmer, D. Liko, T. Madlener, I. Mikulec, N. Rad, H. Rohringer, J. Schieck[1], R. Schöfbeck, M. Spanring, D. Spitzbart, W. Waltenberger, J. Wittmann, C.-E. Wulz[1], M. Zarucki

Institute for Nuclear Problems, Minsk, Belarus
V. Chekhovsky, V. Mossolov, J. Suarez Gonzalez

Universiteit Antwerpen, Antwerpen, Belgium
E.A. De Wolf, D. Di Croce, X. Janssen, J. Lauwers, A. Lelek, M. Pieters, H. Van Haevermaet, P. Van Mechelen, N. Van Remortel

Vrije Universiteit Brussel, Brussel, Belgium
S. Abu Zeid, F. Blekman, J. D'Hondt, J. De Clercq, K. Deroover, G. Flouris, D. Lontkovskyi, S. Lowette, I. Marchesini, S. Moortgat, L. Moreels, Q. Python, K. Skovpen, S. Tavernier, W. Van Doninck, P. Van Mulders, I. Van Parijs

Université Libre de Bruxelles, Bruxelles, Belgium
D. Beghin, B. Bilin, H. Brun, B. Clerbaux, G. De Lentdecker, H. Delannoy, B. Dorney, G. Fasanella, L. Favart, A. Grebenyuk, A.K. Kalsi, T. Lenzi, J. Luetic, N. Postiau, E. Starling, L. Thomas, C. Vander Velde, P. Vanlaer, D. Vannerom, Q. Wang

Ghent University, Ghent, Belgium
T. Cornelis, D. Dobur, A. Fagot, M. Gul, I. Khvastunov[2], D. Poyraz, C. Roskas, D. Trocino, M. Tytgat, W. Verbeke, B. Vermassen, M. Vit, N. Zaganidis

Université Catholique de Louvain, Louvain-la-Neuve, Belgium
H. Bakhshiansohi, O. Bondu, G. Bruno, C. Caputo, P. David, C. Delaere, M. Delcourt, A. Giammanco, G. Krintiras, V. Lemaitre, A. Magitteri, K. Piotrzkowski, A. Saggio, M. Vidal Marono, P. Vischia, J. Zobec

Centro Brasileiro de Pesquisas Fisicas, Rio de Janeiro, Brazil
F.L. Alves, G.A. Alves, G. Correia Silva, C. Hensel, A. Moraes, M.E. Pol, P. Rebello Teles

Universidade do Estado do Rio de Janeiro, Rio de Janeiro, Brazil
E. Belchior Batista Das Chagas, W. Carvalho, J. Chinellato[3], E. Coelho, E.M. Da Costa, G.G. Da Silveira[4], D. De Jesus Damiao, C. De Oliveira Martins, S. Fonseca De Souza, H. Malbouisson, D. Matos Figueiredo, M. Melo De Almeida, C. Mora Herrera, L. Mundim, H. Nogima, W.L. Prado Da Silva, L.J. Sanchez Rosas, A. Santoro, A. Sznajder, M. Thiel, E.J. Tonelli Manganote[3], F. Torres Da Silva De Araujo, A. Vilela Pereira

Universidade Estadual Paulista [a], Universidade Federal do ABC [b], São Paulo, Brazil
S. Ahuja[a], C.A. Bernardes[a], L. Calligaris[a], T.R. Fernandez Perez Tomei[a], E.M. Gregores[b], P.G. Mercadante[b], S.F. Novaes[a], SandraS. Padula[a]

Institute for Nuclear Research and Nuclear Energy, Bulgarian Academy of Sciences, Sofia, Bulgaria
A. Aleksandrov, R. Hadjiiska, P. Iaydjiev, A. Marinov, M. Misheva, M. Rodozov, M. Shopova, G. Sultanov

University of Sofia, Sofia, Bulgaria
A. Dimitrov, L. Litov, B. Pavlov, P. Petkov

Beihang University, Beijing, China
W. Fang[5], X. Gao[5], L. Yuan

Institute of High Energy Physics, Beijing, China
M. Ahmad, J.G. Bian, G.M. Chen, H.S. Chen, M. Chen, Y. Chen, C.H. Jiang, D. Leggat, H. Liao, Z. Liu, S.M. Shaheen[6], A. Spiezia, J. Tao, E. Yazgan, H. Zhang, S. Zhang[6], J. Zhao

State Key Laboratory of Nuclear Physics and Technology, Peking University, Beijing, China
Y. Ban, G. Chen, A. Levin, J. Li, L. Li, Q. Li, Y. Mao, S.J. Qian, D. Wang

Tsinghua University, Beijing, China
Y. Wang

Universidad de Los Andes, Bogota, Colombia
C. Avila, A. Cabrera, C.A. Carrillo Montoya, L.F. Chaparro Sierra, C. Florez, C.F. González Hernández, M.A. Segura Delgado

University of Split, Faculty of Electrical Engineering, Mechanical Engineering and Naval Architecture, Split, Croatia
B. Courbon, N. Godinovic, D. Lelas, I. Puljak, T. Sculac

University of Split, Faculty of Science, Split, Croatia
Z. Antunovic, M. Kovac

Institute Rudjer Boskovic, Zagreb, Croatia
V. Brigljevic, D. Ferencek, K. Kadija, B. Mesic, M. Roguljic, A. Starodumov[7], T. Susa

University of Cyprus, Nicosia, Cyprus
M.W. Ather, A. Attikis, M. Kolosova, G. Mavromanolakis, J. Mousa, C. Nicolaou, F. Ptochos, P.A. Razis, H. Rykaczewski

Charles University, Prague, Czech Republic
M. Finger[8], M. Finger Jr.[8]

Escuela Politecnica Nacional, Quito, Ecuador
E. Ayala

Universidad San Francisco de Quito, Quito, Ecuador
E. Carrera Jarrin

Academy of Scientific Research and Technology of the Arab Republic of Egypt, Egyptian Network of High Energy Physics, Cairo, Egypt
A.A. Abdelalim[9,10], S. Elgammal[11], S. Khalil[10]

National Institute of Chemical Physics and Biophysics, Tallinn, Estonia
S. Bhowmik, A. Carvalho Antunes De Oliveira, R.K. Dewanjee, K. Ehataht, M. Kadastik, M. Raidal, C. Veelken

Department of Physics, University of Helsinki, Helsinki, Finland
P. Eerola, H. Kirschenmann, J. Pekkanen, M. Voutilainen

Helsinki Institute of Physics, Helsinki, Finland
J. Havukainen, J.K. Heikkilä, T. Järvinen, V. Karimäki, R. Kinnunen, T. Lampén, K. Lassila-Perini, S. Laurila, S. Lehti, T. Lindén, M. Lotti, P. Luukka, T. Mäenpää, H. Siikonen, E. Tuominen, J. Tuominiemi

Lappeenranta University of Technology, Lappeenranta, Finland
T. Tuuva

IRFU, CEA, Université Paris-Saclay, Gif-sur-Yvette, France
M. Besancon, F. Couderc, M. Dejardin, D. Denegri, J.L. Faure, F. Ferri, S. Ganjour, A. Givernaud, P. Gras, G. Hamel de Monchenault, P. Jarry, C. Leloup, E. Locci, J. Malcles, G. Negro, J. Rander, A. Rosowsky, M.Ö. Sahin, M. Titov

Laboratoire Leprince-Ringuet, Ecole polytechnique, CNRS/IN2P3, Université Paris-Saclay, Palaiseau, France
A. Abdulsalam[12], C. Amendola, I. Antropov, F. Beaudette, P. Busson, C. Charlot, R. Granier de Cassagnac, I. Kucher, A. Lobanov, J. Martin Blanco, C. Martin Perez, M. Nguyen, C. Ochando, G. Ortona, P. Paganini, J. Rembser, R. Salerno, J.B. Sauvan, Y. Sirois, A.G. Stahl Leiton, A. Zabi, A. Zghiche

Université de Strasbourg, CNRS, IPHC UMR 7178, Strasbourg, France
J.-L. Agram[13], J. Andrea, D. Bloch, G. Bourgatte, J.-M. Brom, E.C. Chabert, V. Cherepanov, C. Collard, E. Conte[13], J.-C. Fontaine[13], D. Gelé, U. Goerlach, M. Jansová, A.-C. Le Bihan, N. Tonon, P. Van Hove

Centre de Calcul de l'Institut National de Physique Nucleaire et de Physique des Particules, CNRS/IN2P3, Villeurbanne, France
S. Gadrat

Université de Lyon, Université Claude Bernard Lyon 1, CNRS-IN2P3, Institut de Physique Nucléaire de Lyon, Villeurbanne, France
S. Beauceron, C. Bernet, G. Boudoul, N. Chanon, R. Chierici, D. Contardo, P. Depasse, H. El Mamouni, J. Fay, L. Finco, S. Gascon, M. Gouzevitch, G. Grenier, B. Ille, F. Lagarde, I.B. Laktineh, H. Lattaud, M. Lethuillier, L. Mirabito, S. Perries, A. Popov[14], V. Sordini, G. Touquet, M. Vander Donckt, S. Viret

Georgian Technical University, Tbilisi, Georgia
T. Toriashvili[15]

Tbilisi State University, Tbilisi, Georgia
Z. Tsamalaidze[8]

RWTH Aachen University, I. Physikalisches Institut, Aachen, Germany
C. Autermann, L. Feld, M.K. Kiesel, K. Klein, M. Lipinski, M. Preuten, M.P. Rauch, C. Schomakers, J. Schulz, M. Teroerde, B. Wittmer

RWTH Aachen University, III. Physikalisches Institut A, Aachen, Germany
A. Albert, M. Erdmann, S. Erdweg, T. Esch, R. Fischer, S. Ghosh, T. Hebbeker, C. Heidemann, K. Hoepfner, H. Keller, L. Mastrolorenzo, M. Merschmeyer, A. Meyer, P. Millet, S. Mukherjee, T. Pook, A. Pozdnyakov, M. Radziej, H. Reithler, M. Rieger, A. Schmidt, D. Teyssier, S. Thüer

RWTH Aachen University, III. Physikalisches Institut B, Aachen, Germany
G. Flügge, O. Hlushchenko, T. Kress, T. Müller, A. Nehrkorn, A. Nowack, C. Pistone, O. Pooth, D. Roy, H. Sert, A. Stahl[16]

Deutsches Elektronen-Synchrotron, Hamburg, Germany
M. Aldaya Martin, T. Arndt, C. Asawatangtrakuldee, I. Babounikau, K. Beernaert, O. Behnke, U. Behrens, A. Bermúdez Martínez, D. Bertsche, A.A. Bin Anuar, K. Borras[17], V. Botta, A. Campbell, P. Connor, C. Contreras-Campana, V. Danilov, A. De Wit, M.M. Defranchis, C. Diez Pardos, D. Domínguez Damiani, G. Eckerlin, T. Eichhorn, A. Elwood, E. Eren, E. Gallo[18], A. Geiser, J.M. Grados Luyando, A. Grohsjean, M. Guthoff, M. Haranko, A. Harb, H. Jung, M. Kasemann, J. Keaveney, C. Kleinwort, J. Knolle, D. Krücker, W. Lange, T. Lenz, J. Leonard, K. Lipka, W. Lohmann[19], R. Mankel, I.-A. Melzer-Pellmann, A.B. Meyer, M. Meyer, M. Missiroli, G. Mittag, J. Mnich, V. Myronenko, S.K. Pflitsch, D. Pitzl, A. Raspereza, A. Saibel, M. Savitskyi, P. Saxena, P. Schütze, C. Schwanenberger, R. Shevchenko, A. Singh, H. Tholen, O. Turkot, A. Vagnerini, M. Van De Klundert, G.P. Van Onsem, R. Walsh, Y. Wen, K. Wichmann, C. Wissing, O. Zenaiev

University of Hamburg, Hamburg, Germany
R. Aggleton, S. Bein, L. Benato, A. Benecke, T. Dreyer, A. Ebrahimi, E. Garutti, D. Gonzalez, P. Gunnellini, J. Haller, A. Hinzmann, A. Karavdina, G. Kasieczka, R. Klanner, R. Kogler, N. Kovalchuk, S. Kurz, V. Kutzner, J. Lange, D. Marconi, J. Multhaup, M. Niedziela, C.E.N. Niemeyer, D. Nowatschin, A. Perieanu, A. Reimers, O. Rieger, C. Scharf, P. Schleper, S. Schumann, J. Schwandt, J. Sonneveld, H. Stadie, G. Steinbrück, F.M. Stober, M. Stöver, B. Vormwald, I. Zoi

Karlsruher Institut fuer Technologie, Karlsruhe, Germany
M. Akbiyik, C. Barth, M. Baselga, S. Baur, E. Butz, R. Caspart, T. Chwalek, F. Colombo, W. De Boer, A. Dierlamm, K. El Morabit, N. Faltermann, B. Freund, M. Giffels, M.A. Harrendorf, F. Hartmann[16], S.M. Heindl, U. Husemann, I. Katkov[14], S. Kudella, S. Mitra, M.U. Mozer, Th. Müller, M. Musich, M. Plagge, G. Quast, K. Rabbertz, M. Schröder, I. Shvetsov, H.J. Simonis, R. Ulrich, S. Wayand, M. Weber, T. Weiler, C. Wöhrmann, R. Wolf

Institute of Nuclear and Particle Physics (INPP), NCSR Demokritos, Aghia Paraskevi, Greece
G. Anagnostou, G. Daskalakis, T. Geralis, A. Kyriakis, D. Loukas, G. Paspalaki

National and Kapodistrian University of Athens, Athens, Greece
A. Agapitos, G. Karathanasis, P. Kontaxakis, A. Panagiotou, I. Papavergou, N. Saoulidou, K. Vellidis

National Technical University of Athens, Athens, Greece
K. Kousouris, I. Papakrivopoulos, G. Tsipolitis

University of Ioánnina, Ioánnina, Greece
I. Evangelou, C. Foudas, P. Gianneios, P. Katsoulis, P. Kokkas, S. Mallios, N. Manthos, I. Papadopoulos, E. Paradas, J. Strologas, F.A. Triantis, D. Tsitsonis

MTA-ELTE Lendület CMS Particle and Nuclear Physics Group, Eötvös Loránd University, Budapest, Hungary
M. Bartók[20], M. Csanad, N. Filipovic, P. Major, M.I. Nagy, G. Pasztor, O. Surányi, G.I. Veres

Wigner Research Centre for Physics, Budapest, Hungary
G. Bencze, C. Hajdu, D. Horvath[21], Á. Hunyadi, F. Sikler, T.Á. Vámi, V. Veszpremi, G. Vesztergombi†

Institute of Nuclear Research ATOMKI, Debrecen, Hungary
N. Beni, S. Czellar, J. Karancsi[20], A. Makovec, J. Molnar, Z. Szillasi

Institute of Physics, University of Debrecen, Debrecen, Hungary
P. Raics, Z.L. Trocsanyi, B. Ujvari

Indian Institute of Science (IISc), Bangalore, India
S. Choudhury, J.R. Komaragiri, P.C. Tiwari

National Institute of Science Education and Research, HBNI, Bhubaneswar, India
S. Bahinipati[23], C. Kar, P. Mal, K. Mandal, A. Nayak[24], S. Roy Chowdhury, D.K. Sahoo[23], S.K. Swain

Panjab University, Chandigarh, India
S. Bansal, S.B. Beri, V. Bhatnagar, S. Chauhan, R. Chawla, N. Dhingra, R. Gupta, A. Kaur, M. Kaur, S. Kaur, P. Kumari, M. Lohan, M. Meena, A. Mehta, K. Sandeep, S. Sharma, J.B. Singh

University of Delhi, Delhi, India
A. Bhardwaj, B.C. Choudhary, R.B. Garg, M. Gola, S. Keshri, Ashok Kumar, S. Malhotra, M. Naimuddin, P. Priyanka, K. Ranjan, Aashaq Shah, R. Sharma

Saha Institute of Nuclear Physics, HBNI, Kolkata, India
R. Bhardwaj[25], M. Bharti[25], R. Bhattacharya, S. Bhattacharya, U. Bhawandeep[25], D. Bhowmik, S. Dey, S. Dutt[25], S. Dutta, S. Ghosh, M. Maity[26], K. Mondal, S. Nandan, A. Purohit, P.K. Rout, A. Roy, G. Saha, S. Sarkar, T. Sarkar[26], M. Sharan, B. Singh[25], S. Thakur[25]

Indian Institute of Technology Madras, Madras, India
P.K. Behera, A. Muhammad

Bhabha Atomic Research Centre, Mumbai, India
R. Chudasama, D. Dutta, V. Jha, V. Kumar, D.K. Mishra, P.K. Netrakanti, L.M. Pant, P. Shukla, P. Suggisetti

Tata Institute of Fundamental Research-A, Mumbai, India
T. Aziz, M.A. Bhat, S. Dugad, G.B. Mohanty, N. Sur, RavindraKumar Verma

Tata Institute of Fundamental Research-B, Mumbai, India
S. Banerjee, S. Bhattacharya, S. Chatterjee, P. Das, M. Guchait, Sa. Jain, S. Karmakar, S. Kumar, G. Majumder, K. Mazumdar, N. Sahoo

Indian Institute of Science Education and Research (IISER), Pune, India
S. Chauhan, S. Dube, V. Hegde, A. Kapoor, K. Kothekar, S. Pandey, A. Rane, A. Rastogi, S. Sharma

Institute for Research in Fundamental Sciences (IPM), Tehran, Iran
S. Chenarani[27], E. Eskandari Tadavani, S.M. Etesami[27], M. Khakzad, M. Mohammadi Najafabadi, M. Naseri, F. Rezaei Hosseinabadi, B. Safarzadeh[28], M. Zeinali

University College Dublin, Dublin, Ireland
M. Felcini, M. Grunewald

INFN Sezione di Bari [a], Università di Bari [b], Politecnico di Bari [c], Bari, Italy
M. Abbrescia[a,b], C. Calabria[a,b], A. Colaleo[a], D. Creanza[a,c], L. Cristella[a,b], N. De Filippis[a,c], M. De Palma[a,b], A. Di Florio[a,b], F. Errico[a,b], L. Fiore[a], A. Gelmi[a,b], G. Iaselli[a,c], M. Ince[a,b], S. Lezki[a,b], G. Maggi[a,c], M. Maggi[a], G. Miniello[a,b], S. My[a,b], S. Nuzzo[a,b], A. Pompili[a,b], G. Pugliese[a,c], R. Radogna[a], A. Ranieri[a], G. Selvaggi[a,b], A. Sharma[a], L. Silvestris[a], R. Venditti[a], P. Verwilligen[a]

INFN Sezione di Bologna [a], Università di Bologna [b], Bologna, Italy
G. Abbiendi[a], C. Battilana[a,b], D. Bonacorsi[a,b], L. Borgonovi[a,b], S. Braibant-Giacomelli[a,b], R. Campanini[a,b], P. Capiluppi[a,b], A. Castro[a,b], F.R. Cavallo[a], S.S. Chhibra[a,b], G. Codispoti[a,b], M. Cuffiani[a,b], G.M. Dallavalle[a], F. Fabbri[a], A. Fanfani[a,b], E. Fontanesi, P. Giacomelli[a], C. Grandi[a], L. Guiducci[a,b], F. Iemmi[a,b], S. Lo Meo[a,29], S. Marcellini[a], G. Masetti[a], A. Montanari[a], F.L. Navarria[a,b], A. Perrotta[a], F. Primavera[a,b], A.M. Rossi[a,b], T. Rovelli[a,b], G.P. Siroli[a,b], N. Tosi[a]

INFN Sezione di Catania [a], Università di Catania [b], Catania, Italy
S. Albergo[a,b], A. Di Mattia[a], R. Potenza[a,b], A. Tricomi[a,b], C. Tuve[a,b]

INFN Sezione di Firenze [a], Università di Firenze [b], Firenze, Italy
G. Barbagli[a], K. Chatterjee[a,b], V. Ciulli[a,b], C. Civinini[a], R. D'Alessandro[a,b], E. Focardi[a,b], G. Latino, P. Lenzi[a,b], M. Meschini[a], S. Paoletti[a], L. Russo[a,30], G. Sguazzoni[a], D. Strom[a], L. Viliani[a]

INFN Laboratori Nazionali di Frascati, Frascati, Italy
L. Benussi, S. Bianco, F. Fabbri, D. Piccolo

INFN Sezione di Genova [a], Università di Genova [b], Genova, Italy
F. Ferro[a], R. Mulargia[a,b], E. Robutti[a], S. Tosi[a,b]

INFN Sezione di Milano-Bicocca [a], Università di Milano-Bicocca [b], Milano, Italy
A. Benaglia[a], A. Beschi[b], F. Brivio[a,b], V. Ciriolo[a,b,16], S. Di Guida[a,b,16], M.E. Dinardo[a,b], S. Fiorendi[a,b], S. Gennai[a], A. Ghezzi[a,b], P. Govoni[a,b], M. Malberti[a,b], S. Malvezzi[a], D. Menasce[a], F. Monti, L. Moroni[a], M. Paganoni[a,b], D. Pedrini[a], S. Ragazzi[a,b], T. Tabarelli de Fatis[a,b], D. Zuolo[a,b]

INFN Sezione di Napoli [a], Università di Napoli 'Federico II' [b], Napoli, Italy, Università della Basilicata [c], Potenza, Italy, Università G. Marconi [d], Roma, Italy
S. Buontempo[a], N. Cavallo[a,c], A. De Iorio[a,b], A. Di Crescenzo[a,b], F. Fabozzi[a,c], F. Fienga[a], G. Galati[a], A.O.M. Iorio[a,b], L. Lista[a], S. Meola[a,d,16], P. Paolucci[a,16], C. Sciacca[a,b], E. Voevodina[a,b]

INFN Sezione di Padova [a], Università di Padova [b], Padova, Italy, Università di Trento [c], Trento, Italy
P. Azzi[a], N. Bacchetta[a], D. Bisello[a,b], A. Boletti[a,b], A. Bragagnolo, R. Carlin[a,b], P. Checchia[a], P. De Castro Manzano[a], T. Dorigo[a], U. Dosselli[a], F. Gasparini[a,b], U. Gasparini[a,b], A. Gozzelino[a], S.Y. Hoh, S. Lacaprara[a], P. Lujan, M. Margoni[a,b], A.T. Meneguzzo[a,b], J. Pazzini[a,b], N. Pozzobon[a,b], M. Presilla[b], P. Ronchese[a,b], R. Rossin[a,b], F. Simonetto[a,b], A. Tiko, E. Torassa[a], M. Tosi[a,b], S. Ventura[a], M. Zanetti[a,b], P. Zotto[a,b]

INFN Sezione di Pavia [a], Università di Pavia [b], Pavia, Italy
A. Braghieri[a], A. Magnani[a], P. Montagna[a,b], S.P. Ratti[a,b], V. Re[a], M. Ressegotti[a,b], C. Riccardi[a,b], P. Salvini[a], I. Vai[a,b], P. Vitulo[a,b]

INFN Sezione di Perugia [a], Università di Perugia [b], Perugia, Italy
M. Biasini[a,b], G.M. Bilei[a], C. Cecchi[a,b], D. Ciangottini[a,b], L. Fanò[a,b], P. Lariccia[a,b], R. Leonardi[a,b], E. Manoni[a], G. Mantovani[a,b], V. Mariani[a,b], M. Menichelli[a], A. Rossi[a,b], A. Santocchia[a,b], D. Spiga[a]

INFN Sezione di Pisa [a], Università di Pisa [b], Scuola Normale Superiore di Pisa [c], Pisa, Italy
K. Androsov[a], P. Azzurri[a], G. Bagliesi[a], L. Bianchini[a], T. Boccali[a], L. Borrello, R. Castaldi[a], M.A. Ciocci[a,b], R. Dell'Orso[a], G. Fedi[a], F. Fiori[a,c], L. Giannini[a,c], A. Giassi[a], M.T. Grippo[a], F. Ligabue[a,c], E. Manca[a,c], G. Mandorli[a,c], A. Messineo[a,b], F. Palla[a], A. Rizzi[a,b], G. Rolandi[31], P. Spagnolo[a], R. Tenchini[a], G. Tonelli[a,b], A. Venturi[a], P.G. Verdini[a]

INFN Sezione di Roma [a], Sapienza Università di Roma [b], Rome, Italy
L. Barone[a,b], F. Cavallari[a], M. Cipriani[a,b], D. Del Re[a,b], E. Di Marco[a,b], M. Diemoz[a], S. Gelli[a,b], E. Longo[a,b], B. Marzocchi[a,b], P. Meridiani[a], G. Organtini[a,b], F. Pandolfi[a], R. Paramatti[a,b], F. Preiato[a,b], S. Rahatlou[a,b], C. Rovelli[a], F. Santanastasio[a,b]

INFN Sezione di Torino [a], Università di Torino [b], Torino, Italy, Università del Piemonte Orientale [c], Novara, Italy
N. Amapane[a,b], R. Arcidiacono[a,c], S. Argiro[a,b], M. Arneodo[a,c], N. Bartosik[a], R. Bellan[a,b], C. Biino[a], A. Cappati[a,b], N. Cartiglia[a], F. Cenna[a,b], S. Cometti[a], M. Costa[a,b], R. Covarelli[a,b], N. Demaria[a], B. Kiani[a,b], C. Mariotti[a], S. Maselli[a], E. Migliore[a,b], V. Monaco[a,b], E. Monteil[a,b], M. Monteno[a], M.M. Obertino[a,b], L. Pacher[a,b], N. Pastrone[a], M. Pelliccioni[a], G.L. Pinna Angioni[a,b], A. Romero[a,b], M. Ruspa[a,c], R. Sacchi[a,b], R. Salvatico[a,b], K. Shchelina[a,b], V. Sola[a], A. Solano[a,b], D. Soldi[a,b], A. Staiano[a]

INFN Sezione di Trieste [a], Università di Trieste [b], Trieste, Italy
S. Belforte[a], V. Candelise[a,b], M. Casarsa[a], F. Cossutti[a], A. Da Rold[a,b], G. Della Ricca[a,b], F. Vazzoler[a,b], A. Zanetti[a]

Kyungpook National University, Daegu, Korea
D.H. Kim, G.N. Kim, M.S. Kim, J. Lee, S.W. Lee, C.S. Moon, Y.D. Oh, S.I. Pak, S. Sekmen, D.C. Son, Y.C. Yang

Chonnam National University, Institute for Universe and Elementary Particles, Kwangju, Korea
H. Kim, D.H. Moon, G. Oh

Hanyang University, Seoul, Korea
B. Francois, J. Goh[32], T.J. Kim

Korea University, Seoul, Korea
S. Cho, S. Choi, Y. Go, D. Gyun, S. Ha, B. Hong, Y. Jo, K. Lee, K.S. Lee, S. Lee, J. Lim, S.K. Park, Y. Roh

Sejong University, Seoul, Korea
H.S. Kim

Seoul National University, Seoul, Korea
J. Almond, J. Kim, J.S. Kim, H. Lee, K. Lee, S. Lee, K. Nam, S.B. Oh, B.C. Radburn-Smith, S.h. Seo, U.K. Yang, H.D. Yoo, G.B. Yu

University of Seoul, Seoul, Korea
D. Jeon, H. Kim, J.H. Kim, J.S.H. Lee, I.C. Park

Sungkyunkwan University, Suwon, Korea
Y. Choi, C. Hwang, J. Lee, I. Yu

Riga Technical University, Riga, Latvia
V. Veckalns[33]

Vilnius University, Vilnius, Lithuania
V. Dudenas, A. Juodagalvis, J. Vaitkus

National Centre for Particle Physics, Universiti Malaya, Kuala Lumpur, Malaysia
Z.A. Ibrahim, M.A.B. Md Ali[34], F. Mohamad Idris[35], W.A.T. Wan Abdullah, M.N. Yusli, Z. Zolkapli

Universidad de Sonora (UNISON), Hermosillo, Mexico
J.F. Benitez, A. Castaneda Hernandez, J.A. Murillo Quijada

Centro de Investigacion y de Estudios Avanzados del IPN, Mexico City, Mexico
H. Castilla-Valdez, E. De La Cruz-Burelo, M.C. Duran-Osuna, I. Heredia-De La Cruz[36], R. Lopez-Fernandez, J. Mejia Guisao, R.I. Rabadan-Trejo, M. Ramirez-Garcia, G. Ramirez-Sanchez, R. Reyes-Almanza, A. Sanchez-Hernandez

Universidad Iberoamericana, Mexico City, Mexico
S. Carrillo Moreno, C. Oropeza Barrera, F. Vazquez Valencia

Benemerita Universidad Autonoma de Puebla, Puebla, Mexico
J. Eysermans, I. Pedraza, H.A. Salazar Ibarguen, C. Uribe Estrada

Universidad Autónoma de San Luis Potosí, San Luis Potosí, Mexico
A. Morelos Pineda

University of Auckland, Auckland, New Zealand
D. Krofcheck

University of Canterbury, Christchurch, New Zealand
S. Bheesette, P.H. Butler

National Centre for Physics, Quaid-I-Azam University, Islamabad, Pakistan
A. Ahmad, M. Ahmad, M.I. Asghar, Q. Hassan, H.R. Hoorani, W.A. Khan, M.A. Shah, M. Shoaib, M. Waqas

National Centre for Nuclear Research, Swierk, Poland
H. Bialkowska, M. Bluj, B. Boimska, T. Frueboes, M. Górski, M. Kazana, M. Szleper, P. Traczyk, P. Zalewski

Institute of Experimental Physics, Faculty of Physics, University of Warsaw, Warsaw, Poland
K. Bunkowski, A. Byszuk[37], K. Doroba, A. Kalinowski, M. Konecki, J. Krolikowski, M. Misiura, M. Olszewski, A. Pyskir, M. Walczak

Laboratório de Instrumentação e Física Experimental de Partículas, Lisboa, Portugal
M. Araujo, P. Bargassa, C. Beirão Da Cruz E Silva, A. Di Francesco, P. Faccioli, B. Galinhas, M. Gallinaro, J. Hollar, N. Leonardo, J. Seixas, G. Strong, O. Toldaiev, J. Varela

Joint Institute for Nuclear Research, Dubna, Russia
S. Afanasiev, P. Bunin, M. Gavrilenko, I. Golutvin, I. Gorbunov, A. Kamenev, V. Karjavine, A. Lanev, A. Malakhov, V. Matveev[38,39], P. Moisenz, V. Palichik, V. Perelygin, S. Shmatov, S. Shulha, N. Skatchkov, V. Smirnov, N. Voytishin, A. Zarubin

Petersburg Nuclear Physics Institute, Gatchina (St. Petersburg), Russia
V. Golovtsov, Y. Ivanov, V. Kim[40], E. Kuznetsova[41], P. Levchenko, V. Murzin, V. Oreshkin, I. Smirnov, D. Sosnov, V. Sulimov, L. Uvarov, S. Vavilov, A. Vorobyev

Institute for Nuclear Research, Moscow, Russia
Yu. Andreev, A. Dermenev, S. Gninenko, N. Golubev, A. Karneyeu, M. Kirsanov, N. Krasnikov, A. Pashenkov, A. Shabanov, D. Tlisov, A. Toropin

Institute for Theoretical and Experimental Physics, Moscow, Russia
V. Epshteyn, V. Gavrilov, N. Lychkovskaya, V. Popov, I. Pozdnyakov, G. Safronov, A. Spiridonov, A. Stepennov, V. Stolin, M. Toms, E. Vlasov, A. Zhokin

Moscow Institute of Physics and Technology, Moscow, Russia
T. Aushev

National Research Nuclear University 'Moscow Engineering Physics Institute' (MEPhI), Moscow, Russia
M. Chadeeva[42], S. Polikarpov[42], E. Popova, V. Rusinov

P.N. Lebedev Physical Institute, Moscow, Russia
V. Andreev, M. Azarkin, I. Dremin[39], M. Kirakosyan, A. Terkulov

Skobeltsyn Institute of Nuclear Physics, Lomonosov Moscow State University, Moscow, Russia
A. Belyaev, E. Boos, V. Bunichev, M. Dubinin[43], L. Dudko, A. Gribushin, V. Klyukhin, O. Kodolova, I. Lokhtin, S. Obraztsov, M. Perfilov, S. Petrushanko, V. Savrin

Novosibirsk State University (NSU), Novosibirsk, Russia
A. Barnyakov[44], V. Blinov[44], T. Dimova[44], L. Kardapoltsev[44], Y. Skovpen[44]

Institute for High Energy Physics of National Research Centre 'Kurchatov Institute', Protvino, Russia
I. Azhgirey, I. Bayshev, S. Bitioukov, V. Kachanov, A. Kalinin, D. Konstantinov, P. Mandrik, V. Petrov, R. Ryutin, S. Slabospitskii, A. Sobol, S. Troshin, N. Tyurin, A. Uzunian, A. Volkov

National Research Tomsk Polytechnic University, Tomsk, Russia
A. Babaev, S. Baidali, V. Okhotnikov

University of Belgrade: Faculty of Physics and VINCA Institute of Nuclear Sciences
P. Adzic[45], P. Cirkovic, D. Devetak, M. Dordevic, P. Milenovic[46], J. Milosevic

Centro de Investigaciones Energéticas Medioambientales y Tecnológicas (CIEMAT), Madrid, Spain
J. Alcaraz Maestre, A. Álvarez Fernández, I. Bachiller, M. Barrio Luna, J.A. Brochero Cifuentes, M. Cerrada, N. Colino, B. De La Cruz, A. Delgado Peris, C. Fernandez Bedoya, J.P. Fernández Ramos, J. Flix, M.C. Fouz, O. Gonzalez Lopez, S. Goy Lopez, J.M. Hernandez, M.I. Josa, D. Moran, A. Pérez-Calero Yzquierdo, J. Puerta Pelayo, I. Redondo, L. Romero, S. Sánchez Navas, M.S. Soares, A. Triossi

Universidad Autónoma de Madrid, Madrid, Spain
C. Albajar, J.F. de Trocóniz

Universidad de Oviedo, Oviedo, Spain
J. Cuevas, C. Erice, J. Fernandez Menendez, S. Folgueras, I. Gonzalez Caballero, J.R. González Fernández, E. Palencia Cortezon, V. Rodríguez Bouza, S. Sanchez Cruz, J.M. Vizan Garcia

Instituto de Física de Cantabria (IFCA), CSIC-Universidad de Cantabria, Santander, Spain
I.J. Cabrillo, A. Calderon, B. Chazin Quero, J. Duarte Campderros, M. Fernandez, P.J. Fernández Manteca, A. García Alonso, J. Garcia-Ferrero, G. Gomez, A. Lopez Virto, J. Marco, C. Martinez Rivero, P. Martinez Ruiz del Arbol, F. Matorras, J. Piedra Gomez, C. Prieels, T. Rodrigo, A. Ruiz-Jimeno, L. Scodellaro, N. Trevisani, I. Vila, R. Vilar Cortabitarte

University of Ruhuna, Department of Physics, Matara, Sri Lanka
N. Wickramage

CERN, European Organization for Nuclear Research, Geneva, Switzerland
D. Abbaneo, B. Akgun, E. Auffray, G. Auzinger, P. Baillon, A.H. Ball, D. Barney, J. Bendavid,

M. Bianco, A. Bocci, C. Botta, E. Brondolin, T. Camporesi, M. Cepeda, G. Cerminara, E. Chapon, Y. Chen, G. Cucciati, D. d'Enterria, A. Dabrowski, N. Daci, V. Daponte, A. David, A. De Roeck, N. Deelen, M. Dobson, M. Dünser, N. Dupont, A. Elliott-Peisert, F. Fallavollita[47], D. Fasanella, G. Franzoni, J. Fulcher, W. Funk, D. Gigi, A. Gilbert, K. Gill, F. Glege, M. Gruchala, M. Guilbaud, D. Gulhan, J. Hegeman, C. Heidegger, Y. Iiyama, V. Innocente, G.M. Innocenti, A. Jafari, P. Janot, O. Karacheban[19], J. Kieseler, A. Kornmayer, M. Krammer[1], C. Lange, P. Lecoq, C. Lourenço, L. Malgeri, M. Mannelli, A. Massironi, F. Meijers, J.A. Merlin, S. Mersi, E. Meschi, F. Moortgat, M. Mulders, J. Ngadiuba, S. Nourbakhsh, S. Orfanelli, L. Orsini, F. Pantaleo[16], L. Pape, E. Perez, M. Peruzzi, A. Petrilli, G. Petrucciani, A. Pfeiffer, M. Pierini, F.M. Pitters, D. Rabady, A. Racz, M. Rovere, H. Sakulin, C. Schäfer, C. Schwick, M. Selvaggi, A. Sharma, P. Silva, P. Sphicas[48], A. Stakia, J. Steggemann, D. Treille, A. Tsirou, A. Vartak, M. Verzetti, W.D. Zeuner

Paul Scherrer Institut, Villigen, Switzerland
L. Caminada[49], K. Deiters, W. Erdmann, R. Horisberger, Q. Ingram, H.C. Kaestli, D. Kotlinski, U. Langenegger, T. Rohe, S.A. Wiederkehr

ETH Zurich - Institute for Particle Physics and Astrophysics (IPA), Zurich, Switzerland
M. Backhaus, L. Bäni, P. Berger, N. Chernyavskaya, G. Dissertori, M. Dittmar, M. Donegà, C. Dorfer, T.A. Gómez Espinosa, C. Grab, D. Hits, T. Klijnsma, W. Lustermann, R.A. Manzoni, M. Marionneau, M.T. Meinhard, F. Micheli, P. Musella, F. Nessi-Tedaldi, F. Pauss, G. Perrin, L. Perrozzi, S. Pigazzini, M. Reichmann, C. Reissel, D. Ruini, D.A. Sanz Becerra, M. Schönenberger, L. Shchutska, V.R. Tavolaro, K. Theofilatos, M.L. Vesterbacka Olsson, R. Wallny, D.H. Zhu

Universität Zürich, Zurich, Switzerland
T.K. Aarrestad, C. Amsler[50], D. Brzhechko, M.F. Canelli, A. De Cosa, R. Del Burgo, S. Donato, C. Galloni, T. Hreus, B. Kilminster, S. Leontsinis, V.M. Mikuni, I. Neutelings, G. Rauco, P. Robmann, D. Salerno, K. Schweiger, C. Seitz, Y. Takahashi, S. Wertz, A. Zucchetta

National Central University, Chung-Li, Taiwan
T.H. Doan, R. Khurana, C.M. Kuo, W. Lin, S.S. Yu

National Taiwan University (NTU), Taipei, Taiwan
P. Chang, Y. Chao, K.F. Chen, P.H. Chen, W.-S. Hou, Y.F. Liu, R.-S. Lu, E. Paganis, A. Psallidas, A. Steen

Chulalongkorn University, Faculty of Science, Department of Physics, Bangkok, Thailand
B. Asavapibhop, N. Srimanobhas, N. Suwonjandee

Çukurova University, Physics Department, Science and Art Faculty, Adana, Turkey
A. Bat, F. Boran, S. Damarseckin, Z.S. Demiroglu, F. Dolek, C. Dozen, I. Dumanoglu, E. Eskut, G. Gokbulut, Y. Guler, E. Gurpinar, I. Hos[51], C. Isik, E.E. Kangal[52], O. Kara, A. Kayis Topaksu, U. Kiminsu, M. Oglakci, G. Onengut, K. Ozdemir[53], A. Polatoz, D. Sunar Cerci[54], B. Tali[54], U.G. Tok, S. Turkcapar, I.S. Zorbakir, C. Zorbilmez

Middle East Technical University, Physics Department, Ankara, Turkey
B. Isildak[55], G. Karapinar[56], M. Yalvac, M. Zeyrek

Bogazici University, Istanbul, Turkey
I.O. Atakisi, E. Gülmez, M. Kaya[57], O. Kaya[58], Ö. Özçelik, S. Ozkorucuklu[59], S. Tekten, E.A. Yetkin[60]

Istanbul Technical University, Istanbul, Turkey
M.N. Agaras, A. Cakir, K. Cankocak, Y. Komurcu, S. Sen[61]

Institute for Scintillation Materials of National Academy of Science of Ukraine, Kharkov, Ukraine
B. Grynyov

National Scientific Center, Kharkov Institute of Physics and Technology, Kharkov, Ukraine
L. Levchuk

University of Bristol, Bristol, United Kingdom
F. Ball, J.J. Brooke, D. Burns, E. Clement, D. Cussans, O. Davignon, H. Flacher, J. Goldstein, G.P. Heath, H.F. Heath, L. Kreczko, D.M. Newbold[62], S. Paramesvaran, B. Penning, T. Sakuma, D. Smith, V.J. Smith, J. Taylor, A. Titterton

Rutherford Appleton Laboratory, Didcot, United Kingdom
K.W. Bell, A. Belyaev[63], C. Brew, R.M. Brown, D. Cieri, D.J.A. Cockerill, J.A. Coughlan, K. Harder, S. Harper, J. Linacre, K. Manolopoulos, E. Olaiya, D. Petyt, T. Reis, T. Schuh, C.H. Shepherd-Themistocleous, A. Thea, I.R. Tomalin, T. Williams, W.J. Womersley

Imperial College, London, United Kingdom
R. Bainbridge, P. Bloch, J. Borg, S. Breeze, O. Buchmuller, A. Bundock, D. Colling, P. Dauncey, G. Davies, M. Della Negra, R. Di Maria, P. Everaerts, G. Hall, G. Iles, T. James, M. Komm, C. Laner, L. Lyons, A.-M. Magnan, S. Malik, A. Martelli, J. Nash[64], A. Nikitenko[7], V. Palladino, M. Pesaresi, D.M. Raymond, A. Richards, A. Rose, E. Scott, C. Seez, A. Shtipliyski, G. Singh, M. Stoye, T. Strebler, S. Summers, A. Tapper, K. Uchida, T. Virdee[16], N. Wardle, D. Winterbottom, J. Wright, S.C. Zenz

Brunel University, Uxbridge, United Kingdom
J.E. Cole, P.R. Hobson, A. Khan, P. Kyberd, C.K. Mackay, A. Morton, I.D. Reid, L. Teodorescu, S. Zahid

Baylor University, Waco, USA
K. Call, J. Dittmann, K. Hatakeyama, H. Liu, C. Madrid, B. McMaster, N. Pastika, C. Smith

Catholic University of America, Washington, DC, USA
R. Bartek, A. Dominguez

The University of Alabama, Tuscaloosa, USA
A. Buccilli, S.I. Cooper, C. Henderson, P. Rumerio, C. West

Boston University, Boston, USA
D. Arcaro, T. Bose, Z. Demiragli, D. Gastler, S. Girgis, D. Pinna, C. Richardson, J. Rohlf, D. Sperka, I. Suarez, L. Sulak, D. Zou

Brown University, Providence, USA
G. Benelli, B. Burkle, X. Coubez, D. Cutts, M. Hadley, J. Hakala, U. Heintz, J.M. Hogan[65], K.H.M. Kwok, E. Laird, G. Landsberg, J. Lee, Z. Mao, M. Narain, S. Sagir[66], R. Syarif, E. Usai, D. Yu

University of California, Davis, Davis, USA
R. Band, C. Brainerd, R. Breedon, D. Burns, M. Calderon De La Barca Sanchez, M. Chertok, J. Conway, R. Conway, P.T. Cox, R. Erbacher, C. Flores, G. Funk, W. Ko, O. Kukral, R. Lander, M. Mulhearn, D. Pellett, J. Pilot, S. Shalhout, M. Shi, D. Stolp, D. Taylor, K. Tos, M. Tripathi, Z. Wang, F. Zhang

University of California, Los Angeles, USA
M. Bachtis, C. Bravo, R. Cousins, A. Dasgupta, S. Erhan, A. Florent, J. Hauser, M. Ignatenko, N. Mccoll, S. Regnard, D. Saltzberg, C. Schnaible, V. Valuev

University of California, Riverside, Riverside, USA
E. Bouvier, K. Burt, R. Clare, J.W. Gary, S.M.A. Ghiasi Shirazi, G. Hanson, G. Karapostoli, E. Kennedy, F. Lacroix, O.R. Long, M. Olmedo Negrete, M.I. Paneva, W. Si, L. Wang, H. Wei, S. Wimpenny, B.R. Yates

University of California, San Diego, La Jolla, USA
J.G. Branson, P. Chang, S. Cittolin, M. Derdzinski, R. Gerosa, D. Gilbert, B. Hashemi, A. Holzner, D. Klein, G. Kole, V. Krutelyov, J. Letts, M. Masciovecchio, S. May, D. Olivito, S. Padhi, M. Pieri, V. Sharma, M. Tadel, J. Wood, F. Würthwein, A. Yagil, G. Zevi Della Porta

University of California, Santa Barbara - Department of Physics, Santa Barbara, USA
N. Amin, R. Bhandari, C. Campagnari, M. Citron, V. Dutta, M. Franco Sevilla, L. Gouskos, R. Heller, J. Incandela, H. Mei, A. Ovcharova, H. Qu, J. Richman, D. Stuart, S. Wang, J. Yoo

California Institute of Technology, Pasadena, USA
D. Anderson, A. Bornheim, J.M. Lawhorn, N. Lu, H.B. Newman, T.Q. Nguyen, J. Pata, M. Spiropulu, J.R. Vlimant, R. Wilkinson, S. Xie, Z. Zhang, R.Y. Zhu

Carnegie Mellon University, Pittsburgh, USA
M.B. Andrews, T. Ferguson, T. Mudholkar, M. Paulini, M. Sun, I. Vorobiev, M. Weinberg

University of Colorado Boulder, Boulder, USA
J.P. Cumalat, W.T. Ford, F. Jensen, A. Johnson, E. MacDonald, T. Mulholland, R. Patel, A. Perloff, K. Stenson, K.A. Ulmer, S.R. Wagner

Cornell University, Ithaca, USA
J. Alexander, J. Chaves, Y. Cheng, J. Chu, A. Datta, K. Mcdermott, N. Mirman, J.R. Patterson, D. Quach, A. Rinkevicius, A. Ryd, L. Skinnari, L. Soffi, S.M. Tan, Z. Tao, J. Thom, J. Tucker, P. Wittich, M. Zientek

Fermi National Accelerator Laboratory, Batavia, USA
S. Abdullin, M. Albrow, M. Alyari, G. Apollinari, A. Apresyan, A. Apyan, S. Banerjee, L.A.T. Bauerdick, A. Beretvas, J. Berryhill, P.C. Bhat, K. Burkett, J.N. Butler, A. Canepa, G.B. Cerati, H.W.K. Cheung, F. Chlebana, M. Cremonesi, J. Duarte, V.D. Elvira, J. Freeman, Z. Gecse, E. Gottschalk, L. Gray, D. Green, S. Grünendahl, O. Gutsche, J. Hanlon, R.M. Harris, S. Hasegawa, J. Hirschauer, Z. Hu, B. Jayatilaka, S. Jindariani, M. Johnson, U. Joshi, B. Klima, M.J. Kortelainen, B. Kreis, S. Lammel, D. Lincoln, R. Lipton, M. Liu, T. Liu, J. Lykken, K. Maeshima, J.M. Marraffino, D. Mason, P. McBride, P. Merkel, S. Mrenna, S. Nahn, V. O'Dell, K. Pedro, C. Pena, O. Prokofyev, G. Rakness, F. Ravera, A. Reinsvold, L. Ristori, A. Savoy-Navarro[67], B. Schneider, E. Sexton-Kennedy, A. Soha, W.J. Spalding, L. Spiegel, S. Stoynev, J. Strait, N. Strobbe, L. Taylor, S. Tkaczyk, N.V. Tran, L. Uplegger, E.W. Vaandering, C. Vernieri, M. Verzocchi, R. Vidal, M. Wang, H.A. Weber

University of Florida, Gainesville, USA
D. Acosta, P. Avery, P. Bortignon, D. Bourilkov, A. Brinkerhoff, L. Cadamuro, A. Carnes, D. Curry, R.D. Field, S.V. Gleyzer, B.M. Joshi, J. Konigsberg, A. Korytov, K.H. Lo, P. Ma, K. Matchev, N. Menendez, G. Mitselmakher, D. Rosenzweig, K. Shi, J. Wang, S. Wang, X. Zuo

Florida International University, Miami, USA
Y.R. Joshi, S. Linn

Florida State University, Tallahassee, USA
A. Ackert, T. Adams, A. Askew, S. Hagopian, V. Hagopian, K.F. Johnson, T. Kolberg, G. Martinez, T. Perry, H. Prosper, A. Saha, C. Schiber, R. Yohay

Florida Institute of Technology, Melbourne, USA
M.M. Baarmand, V. Bhopatkar, S. Colafranceschi, M. Hohlmann, D. Noonan, M. Rahmani, T. Roy, M. Saunders, F. Yumiceva

University of Illinois at Chicago (UIC), Chicago, USA
M.R. Adams, L. Apanasevich, D. Berry, R.R. Betts, R. Cavanaugh, X. Chen, S. Dittmer, O. Evdokimov, C.E. Gerber, D.A. Hangal, D.J. Hofman, K. Jung, J. Kamin, C. Mills, M.B. Tonjes, N. Varelas, H. Wang, X. Wang, Z. Wu, J. Zhang

The University of Iowa, Iowa City, USA
M. Alhusseini, B. Bilki[68], W. Clarida, K. Dilsiz[69], S. Durgut, R.P. Gandrajula, M. Haytmyradov, V. Khristenko, J.-P. Merlo, A. Mestvirishvili, A. Moeller, J. Nachtman, H. Ogul[70], Y. Onel, F. Ozok[71], A. Penzo, C. Snyder, E. Tiras, J. Wetzel

Johns Hopkins University, Baltimore, USA
B. Blumenfeld, A. Cocoros, N. Eminizer, D. Fehling, L. Feng, A.V. Gritsan, W.T. Hung, P. Maksimovic, J. Roskes, U. Sarica, M. Swartz, M. Xiao

The University of Kansas, Lawrence, USA
A. Al-bataineh, P. Baringer, A. Bean, S. Boren, J. Bowen, A. Bylinkin, J. Castle, S. Khalil, A. Kropivnitskaya, D. Majumder, W. Mcbrayer, M. Murray, C. Rogan, S. Sanders, E. Schmitz, J.D. Tapia Takaki, Q. Wang

Kansas State University, Manhattan, USA
S. Duric, A. Ivanov, K. Kaadze, D. Kim, Y. Maravin, D.R. Mendis, T. Mitchell, A. Modak, A. Mohammadi

Lawrence Livermore National Laboratory, Livermore, USA
F. Rebassoo, D. Wright

University of Maryland, College Park, USA
A. Baden, O. Baron, A. Belloni, S.C. Eno, Y. Feng, C. Ferraioli, N.J. Hadley, S. Jabeen, G.Y. Jeng, R.G. Kellogg, J. Kunkle, A.C. Mignerey, S. Nabili, F. Ricci-Tam, M. Seidel, Y.H. Shin, A. Skuja, S.C. Tonwar, K. Wong

Massachusetts Institute of Technology, Cambridge, USA
D. Abercrombie, B. Allen, V. Azzolini, A. Baty, R. Bi, S. Brandt, W. Busza, I.A. Cali, M. D'Alfonso, G. Gomez Ceballos, M. Goncharov, P. Harris, D. Hsu, M. Hu, M. Klute, D. Kovalskyi, Y.-J. Lee, P.D. Luckey, B. Maier, A.C. Marini, C. Mcginn, C. Mironov, S. Narayanan, X. Niu, C. Paus, D. Rankin, C. Roland, G. Roland, Z. Shi, G.S.F. Stephans, K. Sumorok, K. Tatar, D. Velicanu, J. Wang, T.W. Wang, B. Wyslouch

University of Minnesota, Minneapolis, USA
A.C. Benvenuti[†], R.M. Chatterjee, A. Evans, P. Hansen, J. Hiltbrand, Sh. Jain, S. Kalafut, M. Krohn, Y. Kubota, Z. Lesko, J. Mans, R. Rusack, M.A. Wadud

University of Mississippi, Oxford, USA
J.G. Acosta, S. Oliveros

University of Nebraska-Lincoln, Lincoln, USA
E. Avdeeva, K. Bloom, D.R. Claes, C. Fangmeier, F. Golf, R. Gonzalez Suarez, R. Kamalieddin, I. Kravchenko, J. Monroy, J.E. Siado, G.R. Snow, B. Stieger

State University of New York at Buffalo, Buffalo, USA
A. Godshalk, C. Harrington, I. Iashvili, A. Kharchilava, C. Mclean, D. Nguyen, A. Parker, S. Rappoccio, B. Roozbahani

Northeastern University, Boston, USA
G. Alverson, E. Barberis, C. Freer, Y. Haddad, A. Hortiangtham, G. Madigan, D.M. Morse, T. Orimoto, A. Tishelman-charny, T. Wamorkar, B. Wang, A. Wisecarver, D. Wood

Northwestern University, Evanston, USA
S. Bhattacharya, J. Bueghly, O. Charaf, T. Gunter, K.A. Hahn, N. Odell, M.H. Schmitt, K. Sung, M. Trovato, M. Velasco

University of Notre Dame, Notre Dame, USA
R. Bucci, N. Dev, R. Goldouzian, M. Hildreth, K. Hurtado Anampa, C. Jessop, D.J. Karmgard, K. Lannon, W. Li, N. Loukas, N. Marinelli, F. Meng, C. Mueller, Y. Musienko[38], M. Planer, R. Ruchti, P. Siddireddy, G. Smith, S. Taroni, M. Wayne, A. Wightman, M. Wolf, A. Woodard

The Ohio State University, Columbus, USA
J. Alimena, L. Antonelli, B. Bylsma, L.S. Durkin, S. Flowers, B. Francis, C. Hill, W. Ji, A. Lefeld, T.Y. Ling, W. Luo, B.L. Winer

Princeton University, Princeton, USA
S. Cooperstein, G. Dezoort, P. Elmer, J. Hardenbrook, N. Haubrich, S. Higginbotham, A. Kalogeropoulos, S. Kwan, D. Lange, M.T. Lucchini, J. Luo, D. Marlow, K. Mei, I. Ojalvo, J. Olsen, C. Palmer, P. Piroué, J. Salfeld-Nebgen, D. Stickland, C. Tully

University of Puerto Rico, Mayaguez, USA
S. Malik, S. Norberg

Purdue University, West Lafayette, USA
A. Barker, V.E. Barnes, S. Das, L. Gutay, M. Jones, A.W. Jung, A. Khatiwada, B. Mahakud, D.H. Miller, N. Neumeister, C.C. Peng, S. Piperov, H. Qiu, J.F. Schulte, J. Sun, F. Wang, R. Xiao, W. Xie

Purdue University Northwest, Hammond, USA
T. Cheng, J. Dolen, N. Parashar

Rice University, Houston, USA
Z. Chen, K.M. Ecklund, S. Freed, F.J.M. Geurts, M. Kilpatrick, Arun Kumar, W. Li, B.P. Padley, R. Redjimi, J. Roberts, J. Rorie, W. Shi, Z. Tu, A. Zhang

University of Rochester, Rochester, USA
A. Bodek, P. de Barbaro, R. Demina, Y.t. Duh, J.L. Dulemba, C. Fallon, T. Ferbel, M. Galanti, A. Garcia-Bellido, J. Han, O. Hindrichs, A. Khukhunaishvili, E. Ranken, P. Tan, R. Taus

Rutgers, The State University of New Jersey, Piscataway, USA
B. Chiarito, J.P. Chou, Y. Gershtein, E. Halkiadakis, A. Hart, M. Heindl, E. Hughes, S. Kaplan, R. Kunnawalkam Elayavalli, S. Kyriacou, I. Laflotte, A. Lath, R. Montalvo, K. Nash, M. Osherson, H. Saka, S. Salur, S. Schnetzer, D. Sheffield, S. Somalwar, R. Stone, S. Thomas, P. Thomassen

University of Tennessee, Knoxville, USA
H. Acharya, A.G. Delannoy, J. Heideman, G. Riley, S. Spanier

Texas A&M University, College Station, USA
O. Bouhali[72], A. Celik, M. Dalchenko, M. De Mattia, A. Delgado, S. Dildick, R. Eusebi, J. Gilmore, T. Huang, T. Kamon[73], S. Luo, D. Marley, R. Mueller, D. Overton, L. Perniè, D. Rathjens, A. Safonov

Texas Tech University, Lubbock, USA
N. Akchurin, J. Damgov, F. De Guio, P.R. Dudero, S. Kunori, K. Lamichhane, S.W. Lee, T. Mengke, S. Muthumuni, T. Peltola, S. Undleeb, I. Volobouev, Z. Wang, A. Whitbeck

Vanderbilt University, Nashville, USA
S. Greene, A. Gurrola, R. Janjam, W. Johns, C. Maguire, A. Melo, H. Ni, K. Padeken, F. Romeo, P. Sheldon, S. Tuo, J. Velkovska, M. Verweij, Q. Xu

University of Virginia, Charlottesville, USA
M.W. Arenton, P. Barria, B. Cox, R. Hirosky, M. Joyce, A. Ledovskoy, H. Li, C. Neu, T. Sinthuprasith, Y. Wang, E. Wolfe, F. Xia

Wayne State University, Detroit, USA
R. Harr, P.E. Karchin, N. Poudyal, J. Sturdy, P. Thapa, S. Zaleski

University of Wisconsin - Madison, Madison, WI, USA
J. Buchanan, C. Caillol, D. Carlsmith, S. Dasu, I. De Bruyn, L. Dodd, B. Gomber[74], M. Grothe, M. Herndon, A. Hervé, U. Hussain, P. Klabbers, A. Lanaro, K. Long, R. Loveless, T. Ruggles, A. Savin, V. Sharma, N. Smith, W.H. Smith, N. Woods

†: Deceased
1: Also at Vienna University of Technology, Vienna, Austria
2: Also at IRFU, CEA, Université Paris-Saclay, Gif-sur-Yvette, France
3: Also at Universidade Estadual de Campinas, Campinas, Brazil
4: Also at Federal University of Rio Grande do Sul, Porto Alegre, Brazil
5: Also at Université Libre de Bruxelles, Bruxelles, Belgium
6: Also at University of Chinese Academy of Sciences, Beijing, China
7: Also at Institute for Theoretical and Experimental Physics, Moscow, Russia
8: Also at Joint Institute for Nuclear Research, Dubna, Russia
9: Also at Helwan University, Cairo, Egypt
10: Now at Zewail City of Science and Technology, Zewail, Egypt
11: Now at British University in Egypt, Cairo, Egypt
12: Also at Department of Physics, King Abdulaziz University, Jeddah, Saudi Arabia
13: Also at Université de Haute Alsace, Mulhouse, France
14: Also at Skobeltsyn Institute of Nuclear Physics, Lomonosov Moscow State University, Moscow, Russia
15: Also at Tbilisi State University, Tbilisi, Georgia
16: Also at CERN, European Organization for Nuclear Research, Geneva, Switzerland
17: Also at RWTH Aachen University, III. Physikalisches Institut A, Aachen, Germany
18: Also at University of Hamburg, Hamburg, Germany
19: Also at Brandenburg University of Technology, Cottbus, Germany
20: Also at Institute of Physics, University of Debrecen, Debrecen, Hungary
21: Also at Institute of Nuclear Research ATOMKI, Debrecen, Hungary
22: Also at MTA-ELTE Lendület CMS Particle and Nuclear Physics Group, Eötvös Loránd University, Budapest, Hungary

23: Also at Indian Institute of Technology Bhubaneswar, Bhubaneswar, India
24: Also at Institute of Physics, Bhubaneswar, India
25: Also at Shoolini University, Solan, India
26: Also at University of Visva-Bharati, Santiniketan, India
27: Also at Isfahan University of Technology, Isfahan, Iran
28: Also at Plasma Physics Research Center, Science and Research Branch, Islamic Azad University, Tehran, Iran
29: Also at ITALIAN NATIONAL AGENCY FOR NEW TECHNOLOGIES, ENERGY AND SUSTAINABLE ECONOMIC DEVELOPMENT, Bologna, Italy
30: Also at Università degli Studi di Siena, Siena, Italy
31: Also at Scuola Normale e Sezione dell'INFN, Pisa, Italy
32: Also at Kyung Hee University, Department of Physics, Seoul, Korea
33: Also at Riga Technical University, Riga, Latvia
34: Also at International Islamic University of Malaysia, Kuala Lumpur, Malaysia
35: Also at Malaysian Nuclear Agency, MOSTI, Kajang, Malaysia
36: Also at Consejo Nacional de Ciencia y Tecnología, Mexico City, Mexico
37: Also at Warsaw University of Technology, Institute of Electronic Systems, Warsaw, Poland
38: Also at Institute for Nuclear Research, Moscow, Russia
39: Now at National Research Nuclear University 'Moscow Engineering Physics Institute' (MEPhI), Moscow, Russia
40: Also at St. Petersburg State Polytechnical University, St. Petersburg, Russia
41: Also at University of Florida, Gainesville, USA
42: Also at P.N. Lebedev Physical Institute, Moscow, Russia
43: Also at California Institute of Technology, Pasadena, USA
44: Also at Budker Institute of Nuclear Physics, Novosibirsk, Russia
45: Also at Faculty of Physics, University of Belgrade, Belgrade, Serbia
46: Also at University of Belgrade, Belgrade, Serbia
47: Also at INFN Sezione di Pavia [a], Università di Pavia [b], Pavia, Italy
48: Also at National and Kapodistrian University of Athens, Athens, Greece
49: Also at Universität Zürich, Zurich, Switzerland
50: Also at Stefan Meyer Institute for Subatomic Physics (SMI), Vienna, Austria
51: Also at Istanbul Aydin University, Istanbul, Turkey
52: Also at Mersin University, Mersin, Turkey
53: Also at Piri Reis University, Istanbul, Turkey
54: Also at Adiyaman University, Adiyaman, Turkey
55: Also at Ozyegin University, Istanbul, Turkey
56: Also at Izmir Institute of Technology, Izmir, Turkey
57: Also at Marmara University, Istanbul, Turkey
58: Also at Kafkas University, Kars, Turkey
59: Also at Istanbul University, Istanbul, Turkey
60: Also at Istanbul Bilgi University, Istanbul, Turkey
61: Also at Hacettepe University, Ankara, Turkey
62: Also at Rutherford Appleton Laboratory, Didcot, United Kingdom
63: Also at School of Physics and Astronomy, University of Southampton, Southampton, United Kingdom
64: Also at Monash University, Faculty of Science, Clayton, Australia
65: Also at Bethel University, St. Paul, USA
66: Also at Karamanoğlu Mehmetbey University, Karaman, Turkey
67: Also at Purdue University, West Lafayette, USA

68: Also at Beykent University, Istanbul, Turkey
69: Also at Bingol University, Bingol, Turkey
70: Also at Sinop University, Sinop, Turkey
71: Also at Mimar Sinan University, Istanbul, Istanbul, Turkey
72: Also at Texas A&M University at Qatar, Doha, Qatar
73: Also at Kyungpook National University, Daegu, Korea
74: Also at University of Hyderabad, Hyderabad, India